Search for $\mu^+ \rightarrow e^+ \gamma$ in the MEG II Experiment's First Physics Dataset

Dylan Palo on Behalf of the MEG II Collaboration
Formerly at University of California, Irvine
Presently at Fermilab

Overview

- Goal:
  - Describe the MEG II experimental technique and its first physics analysis
- Discuss:
  - Theoretical background
  - Experimental overview
  - Physics analysis

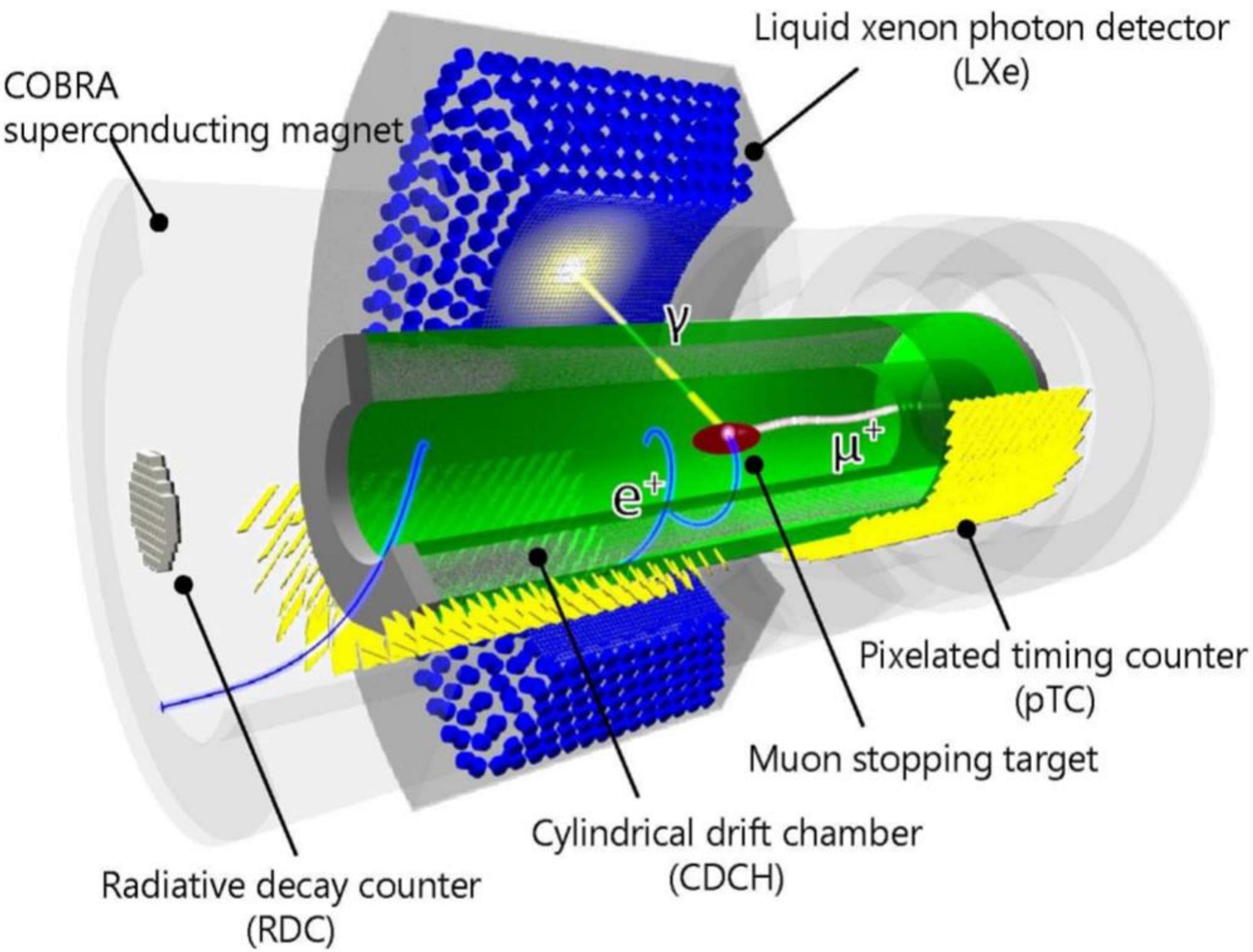

μ→eγ Decay

- No instance of CLFV has been observed
- e.g. μ→eγ decay is possible in SM:
  BR is negligible $\sim 10^{-54}$; $\propto [\frac{(\Delta m_\nu^2)}{m_W^2}]^2$
- BTSM theories allow for CLFV and μ→eγ at higher, detectable rates
  (e.g. SUSY, BR~ 10^{-11}: 10^{-15})
- **MEG II searches for μ→eγ; signal would be clear indication of new physics**

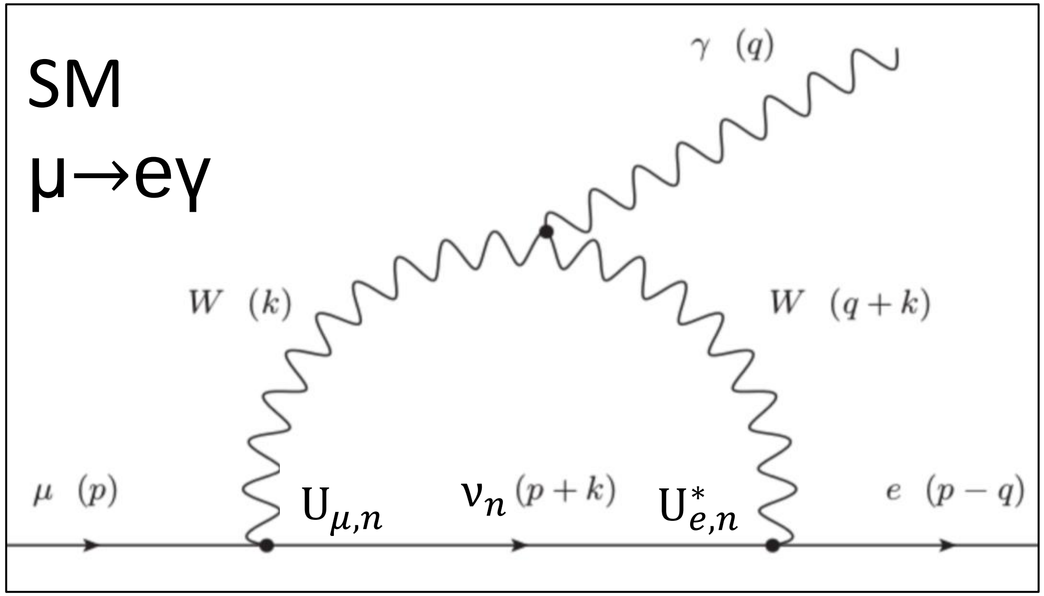

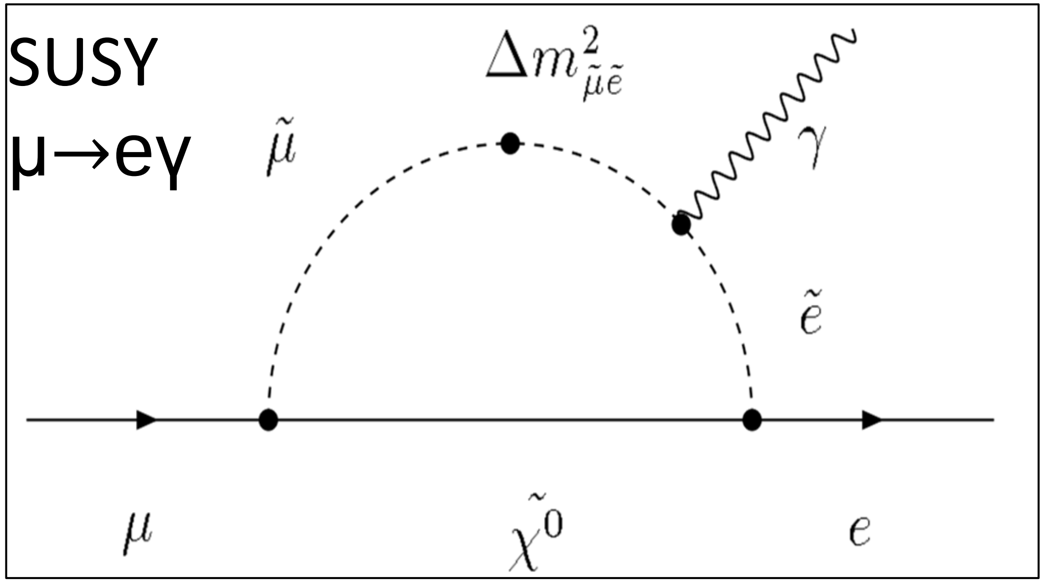

Charged Lepton Violating Theoretical Models

Supersymmetry

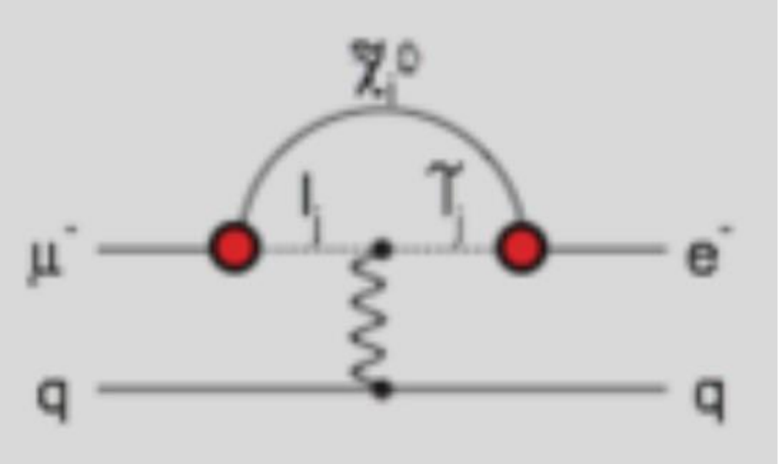

Compositeness

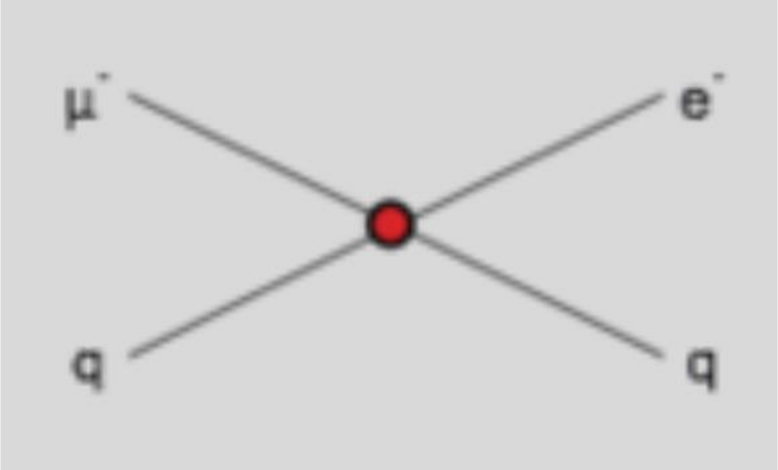

Leptoquark

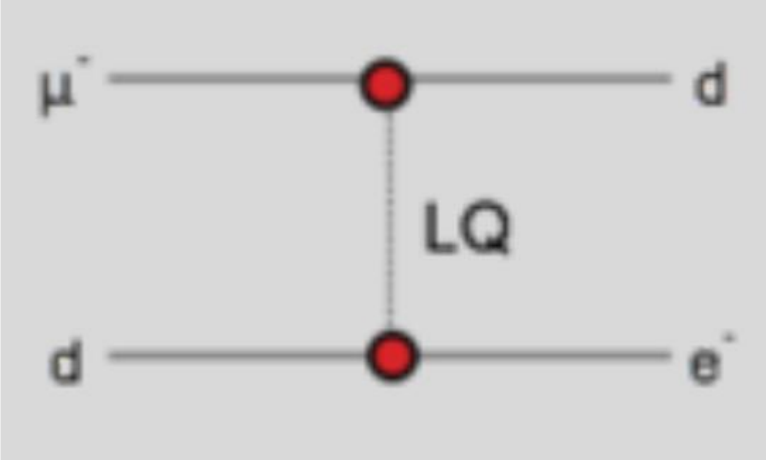

Heavy Neutrinos

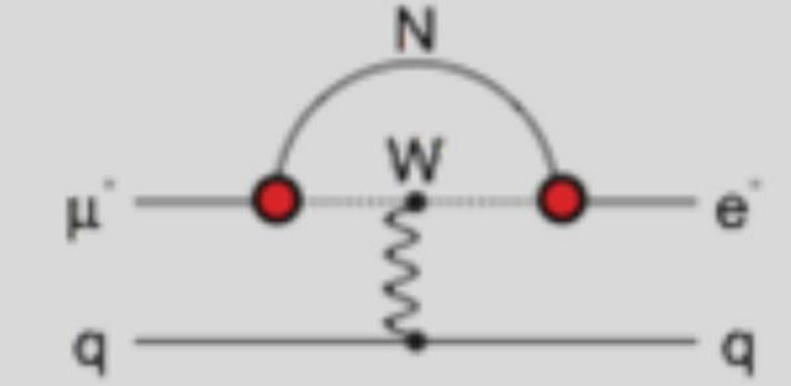

Second Higgs Doublet

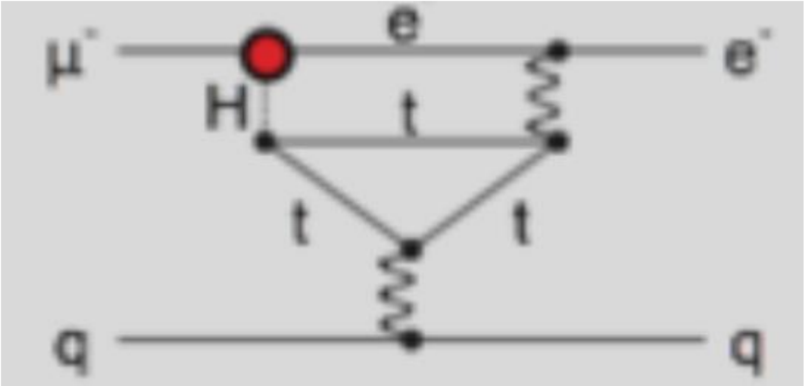

Heavy Z' Anomal. Z Coupling

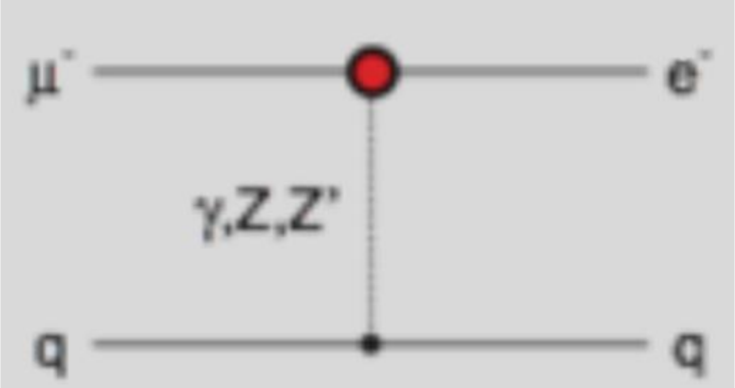

Slide originally by Bill Marciano

CLFV History

- MEG II is the latest in a long line of CLFV experimental searches with others following soon
  e.g. Mu3e, COMET, Mu2e
- Improvements from improved accelerators, detector technology, and experience
- The current μ→eγ decay limit is 4.2x10^{-13} (90% CL), set by MEG I
- **The MEG II collaboration aims to detect μ→eγ or improve upon the sensitivity limit by ~10**

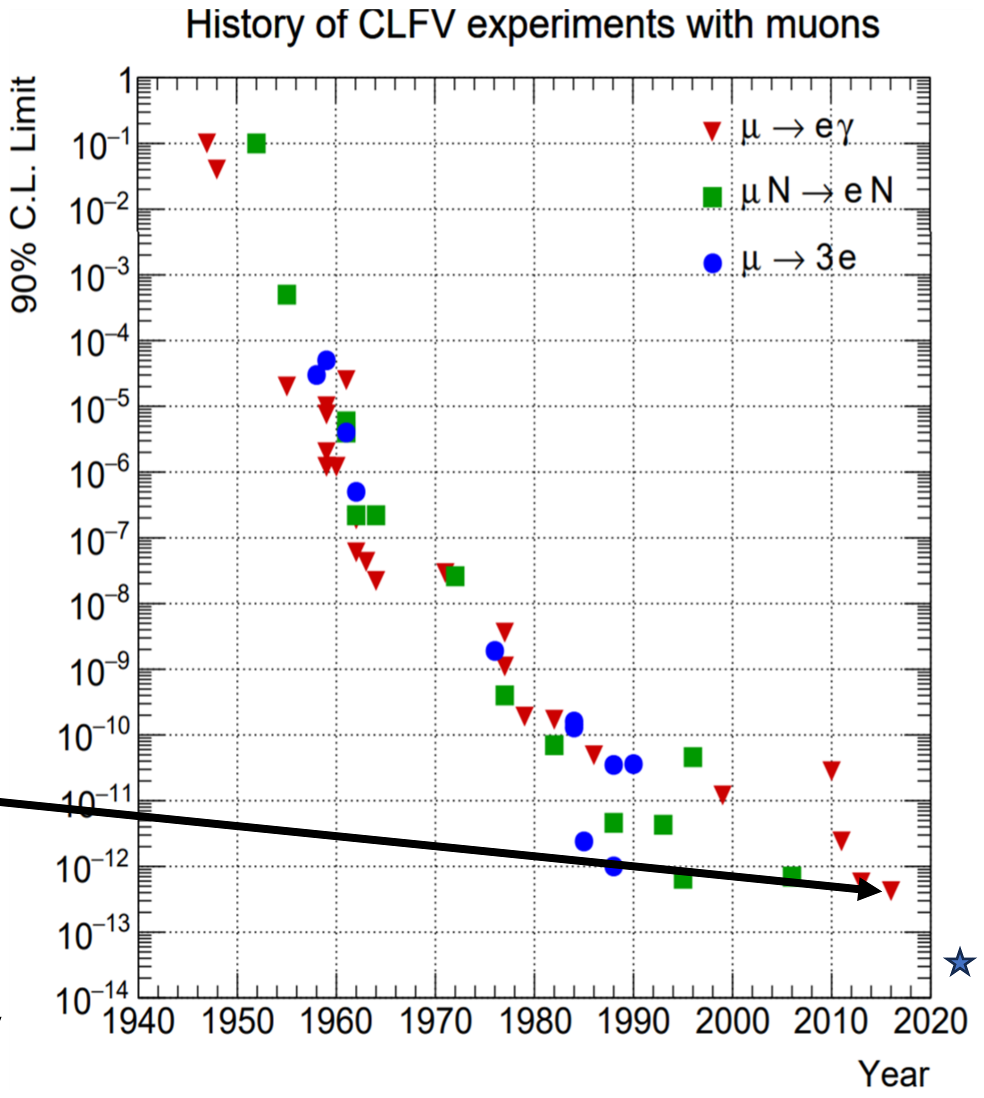

Reaction	Current bound
$\mathcal{B}(\mu^+ \to e^+\gamma)$	$<1.2 \times 10^{-11}$
$\mathcal{B}(\mu^\pm \to e^\pm e^+ e^-)$	$<1.0 \times 10^{-12}$
$\mathcal{B}(\mu^\pm \to e^\pm \gamma\gamma)$	$<7.2 \times 10^{-11}$
$R(\mu^- \mathrm{Au} \to e^- \mathrm{Au})$	$<7 \times 10^{-13}$
$R(\mu^- \mathrm{Al} \to e^- \mathrm{Al})$	–
$\mathcal{B}(\tau^\pm \to \mu^\pm \gamma)$	$<5.9 \times 10^{-8}$
$\mathcal{B}(\tau^\pm \to e^\pm \gamma)$	$<8.5 \times 10^{-8}$
$\mathcal{B}(\tau^\pm \to \mu^\pm \mu^+ \mu^-)$	$<2.0 \times 10^{-8}$
$\mathcal{B}(\tau^\pm \to e^\pm e^+ e^-)$	$<2.6 \times 10^{-8}$
$Z^0 \to e^\pm \mu^\mp$	$<1.7 \times 10^{-6}$
$Z^0 \to e^\pm \tau^\mp$	$<9.8 \times 10^{-6}$
$Z^0 \to \mu^\pm \tau^\mp$	$<1.2 \times 10^{-5}$
$K_L^0 \to e^\pm \mu^\mp$	$<4.7 \times 10^{-12}$
$D^0 \to e^\pm \mu^\mp$	$<8.1 \times 10^{-7}$
$B^0 \to e^\pm \mu^\mp$	$<9.2 \times 10^{-8}$

MEG II Experimental Overview

MEG II Experiment

- International collaboration of ~ 60 physicists
- Based at Paul Scherrer Institut located in Villigen, CH near Zurich
- Uses the PSI proton ring cyclotron
  - 590 MeV protons
  - Unbunched surface muon beam produced: Stop rate ≈ 4×10^7 Hz, 28 MeV muons

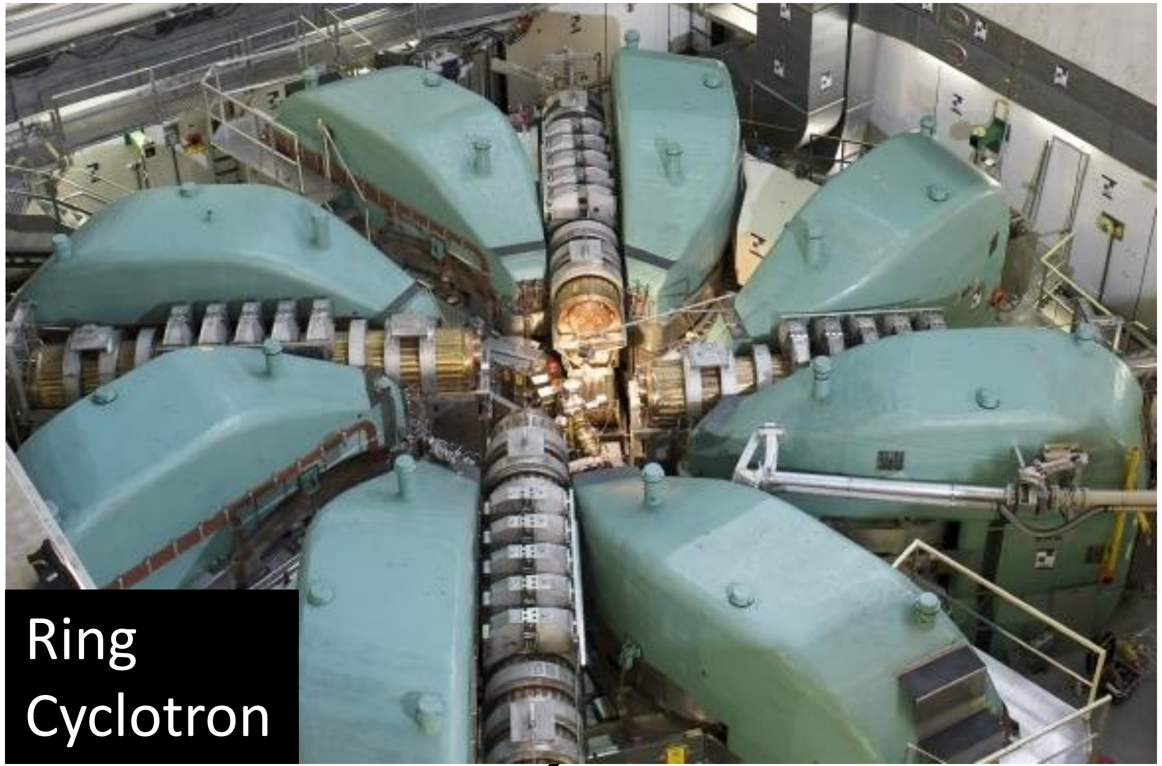

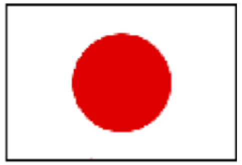

UTokyo
KEK
Kobe

INFN Genoa
INFN Lecce
INFN Pavia
INFN Pisa
INFN Roma

UC Irvine

BINP
JINR

PSI
ETHZ

MEG II Experiment: Signal/Background

- The μ→eγ signal is a two-body decay at rest, signal e/γ have equal and opposite momentum (m_μ/2)
- Background does not have these characteristics:
  - RMD (radiative muon decay) **:** μ^+ →γ $e^+$$\nu_\mu$ $\overline{\nu_e}$ (small E ν_μ $\overline{\nu_e}$)
  - **Accidental background**: high p_{e_+} coincident with γ from RMD, AIF ($e^+\ e^- \rightarrow \gamma\gamma$)
- **The experiment requires precise kinematic measurements of the decay products** to distinguish between signal/background decays

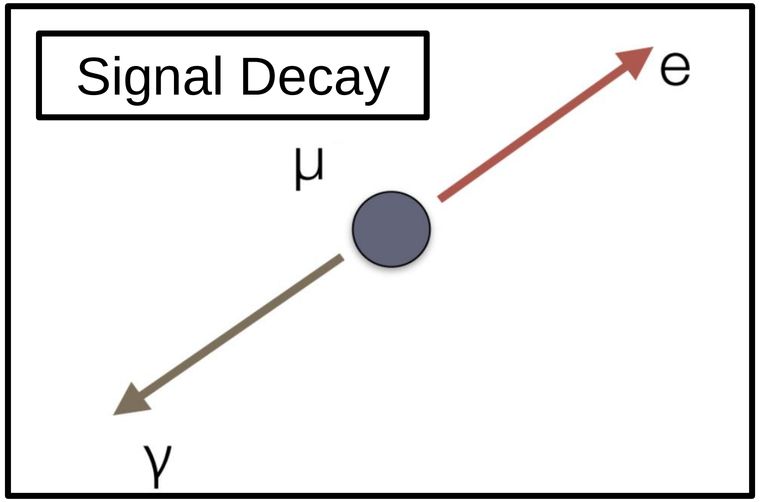

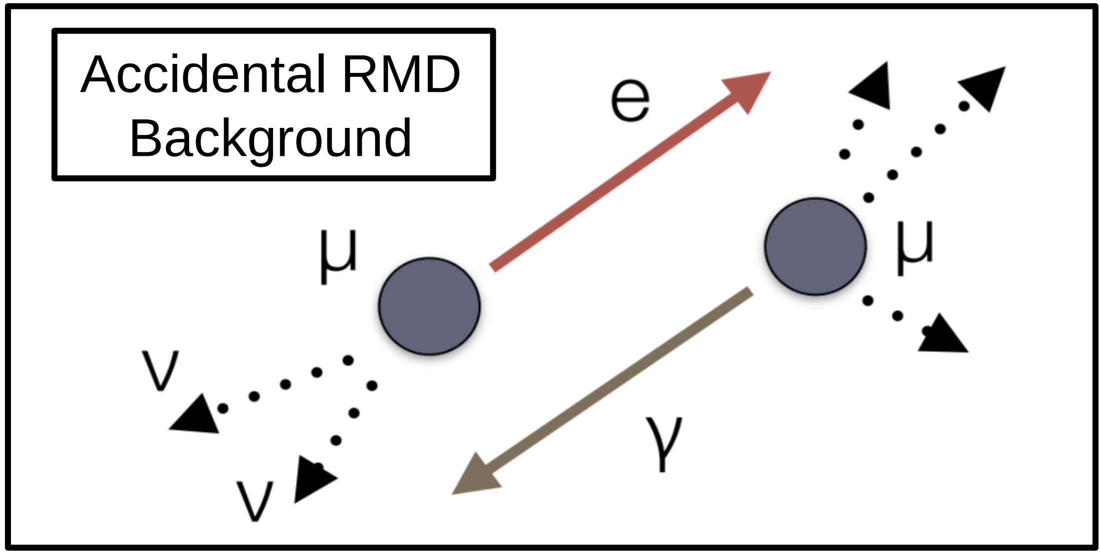

MEG II Experiment: Apparatus

- Stopped μ^+ decay in target; decay products (e, γ) are measured in various detectors
- Similar design to MEG I, but all detectors have been upgraded
- Kinematic estimates at target by propagating e^+ to the target, then projecting γ to e^+ target vertex ($\Delta\theta_{e^+\gamma}, \Delta\varphi_{e^+\gamma}, \Delta t_{e^+\gamma}, E_\gamma, p_{e^+}$)

$$N_{acc} \propto R_{\mu^+}^2 \bullet \Delta E_\gamma^2 \bullet \Delta p_{e^+} \bullet \Delta\varphi_{e^+\gamma} \bullet \Delta\theta_{e^+\gamma} \bullet \Delta t_{e^+\gamma} \bullet \mathrm{T}$$

Max B~1.3 T

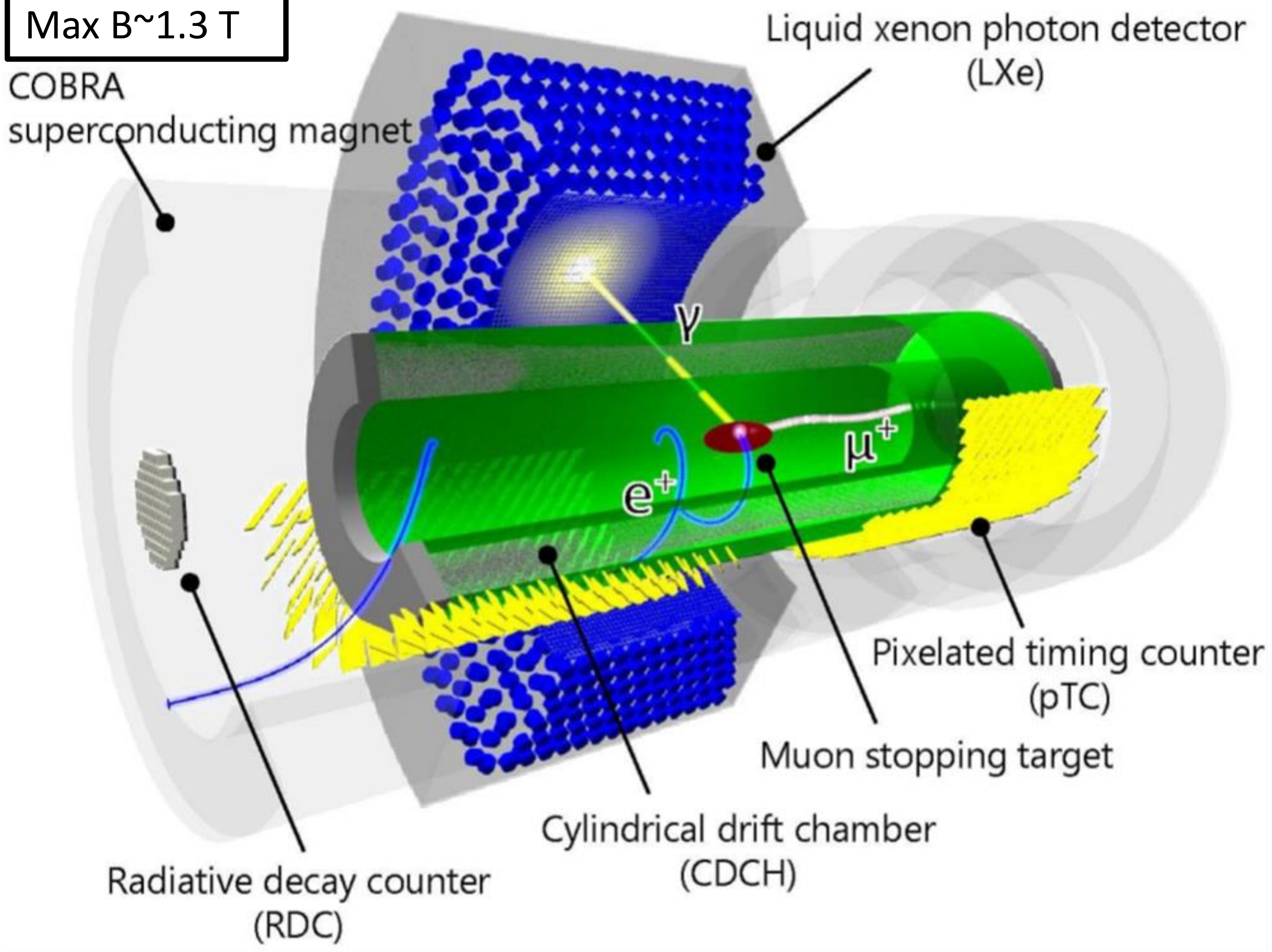

CDCH Detector

- Upgrades:
  - New ultra-light open cell stereo drift chamber to improve efficiency and resolution
  - More track space points in drift chamber to improve resolution (1150 readout drift cells)
- The chamber was filled with $He:C_4H_{10}:C_3H_8O:O_2$ (88.2:9.8:1.5:0.5)
- High voltage wires surrounding sense wire creates drift cell geometry

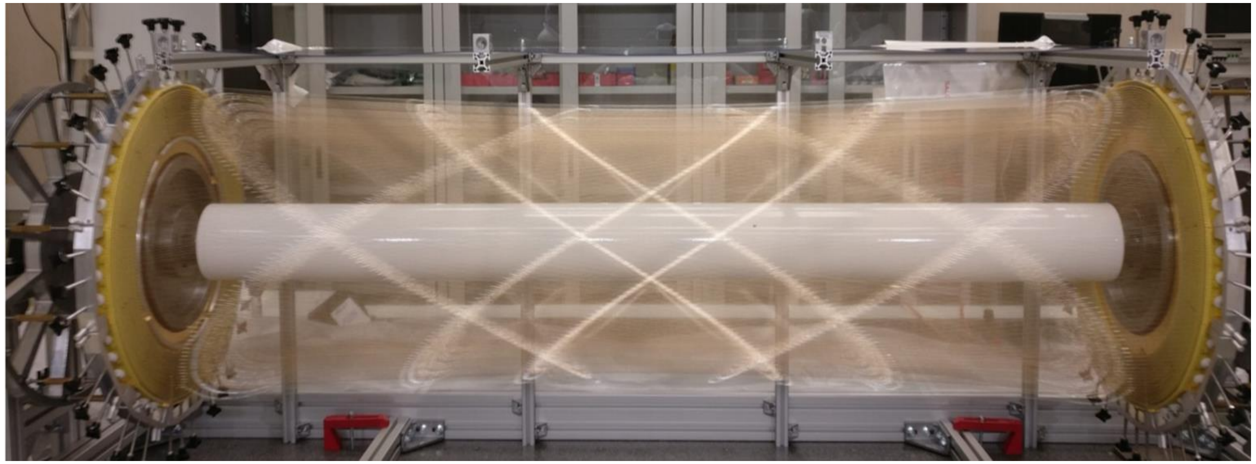

Kinematic Core σ	MEG I	MEG II Goal
p_{e_+}(keV)	**380**	**130**
θ_{e+} /φ_{e+} (mrad)	**9.4 / 8.7***	**5.3/3.7***
t_{e+} (ps)	70	30
z_{e+} /y_{e+} (mm)	**2.4/1.2**	**1.6/0.7**
e+ Efficiency	**30**	**70**

*φ_{e+} estimated at plane perpendicular to track

Time-Distance Isochrones[ns]

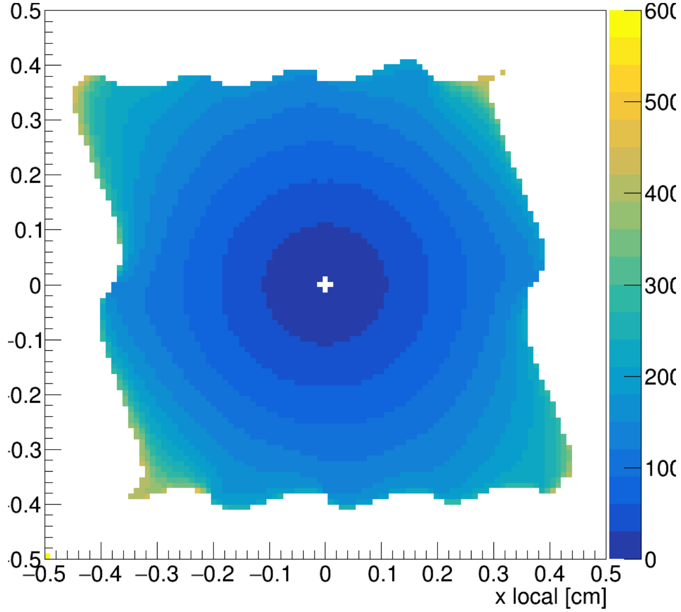

Wire Positions at Chamber Center

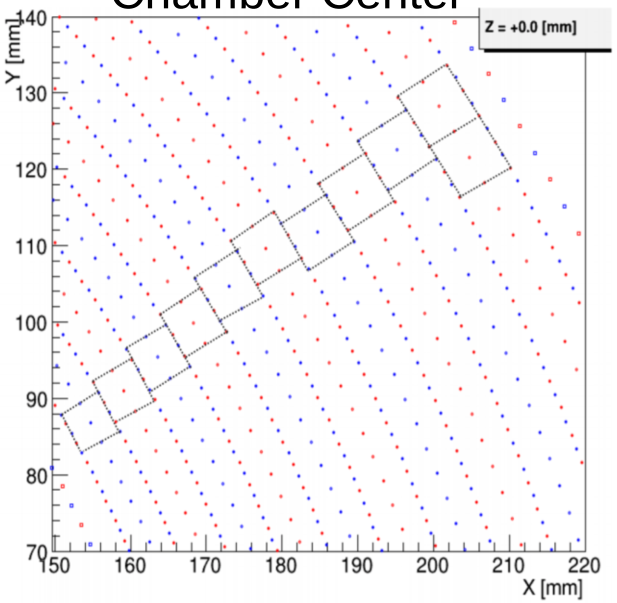

pTC Detector

- Upgrade: new design with higher hit multiplicity
- Two semi-cylindrical modules, each consisting of 256 timing counters
- Counter consists of a scintillation tile with double-sided SiPM readout
- Individual counter timing precision ~90 ps
- Signal e_+ $<N_{TC}>$ ~9; $\sigma_{t_{e^+}}$=30 ps

Kinematic Core σ	MEG I	MEG II Goal
p_{e_+}(keV)	380	130
θ_{e+} /φ_{e+} (mrad)	9.4 / 8.7	5.3/3.7
t_{e+} (ps)	**70**	**30**
z_{e+} /y_{e+} (mm)	2.4/1.2	1.6/0.7
e+ Efficiency	30	70

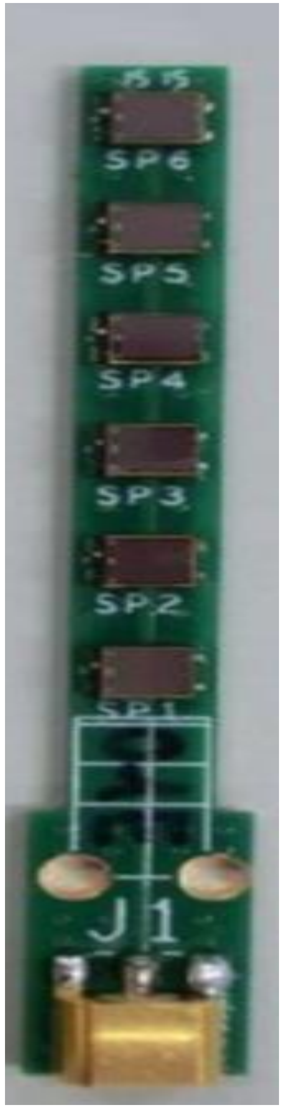

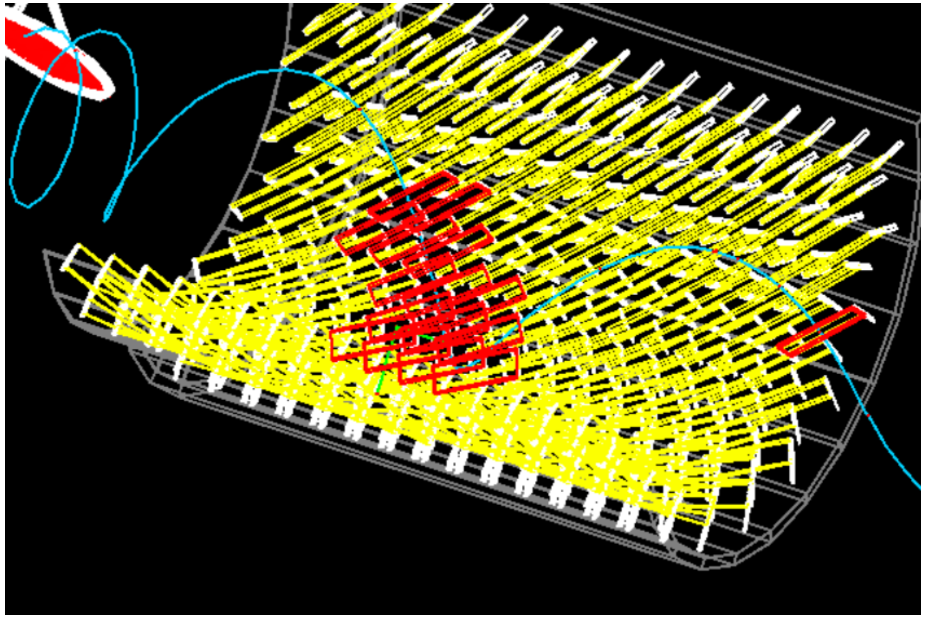

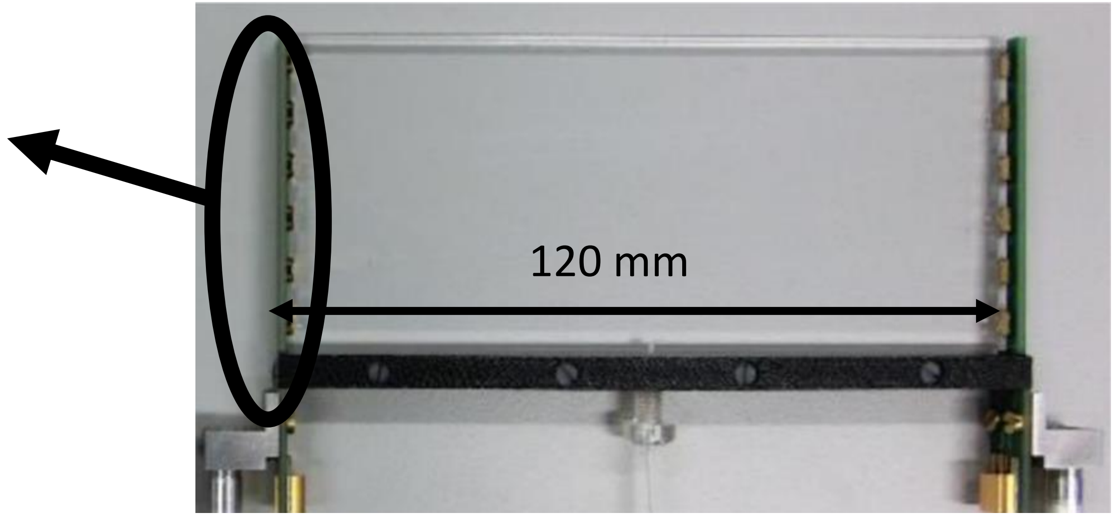

LXe Detector

- One of world's largest liquid Xe detector (800 L)
- Upgrade: inner face PMTs replaced by 4092 15x15mm^2 MPPCs (Multi-Pixel Photon Counters)
- Other 5 sides remain covered by PMT photon counters

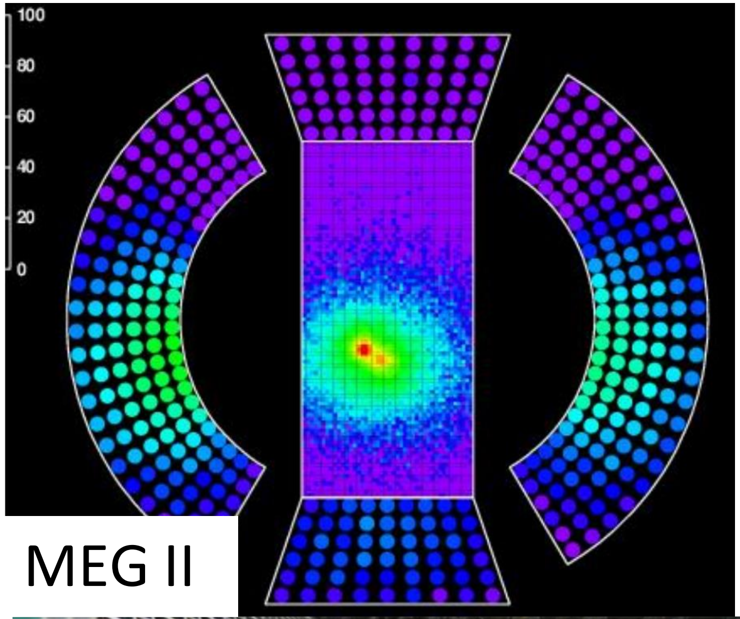

Kinematic Core σ	MEG I	MEG II Goal
E_γ (%)	**2.4**	**1.1**
u_γ (z_γ) (mm)	**5**	**2.6**
v_γ ($R\varphi_\gamma$) (mm)	**5**	**2.2**
w_γ (R_γ) (mm)	**6**	**5**
t_γ (ps)	**60**	**60**

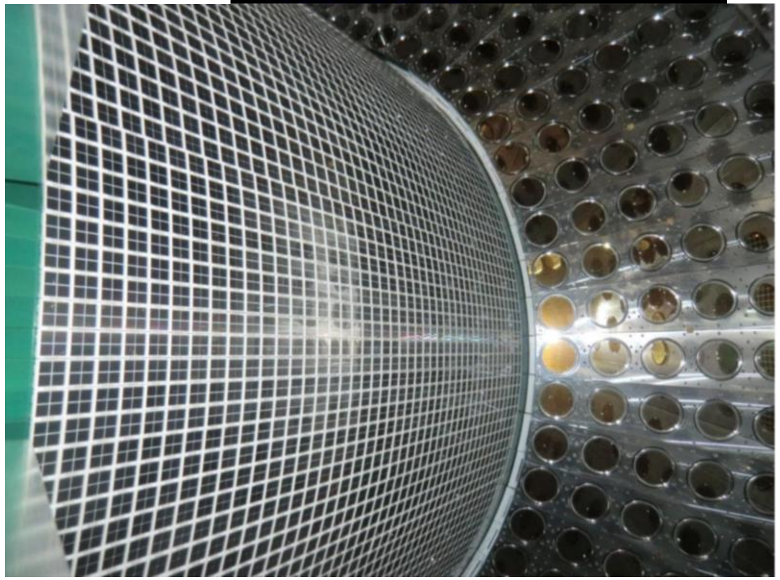

LXe Detector

- One of world’s largest liquid Xe detector (800 L)
- Upgrade: inner face PMTs replaced by 4092 15x15mm^2 MPPCs (Multi-Pixel Photon Counters)
- Other 5 sides remain covered by PMT photon counters

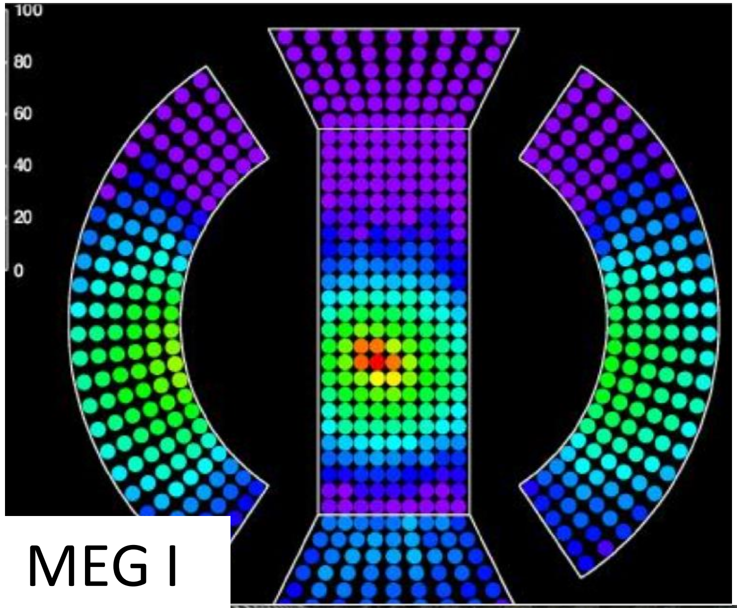

MEG I

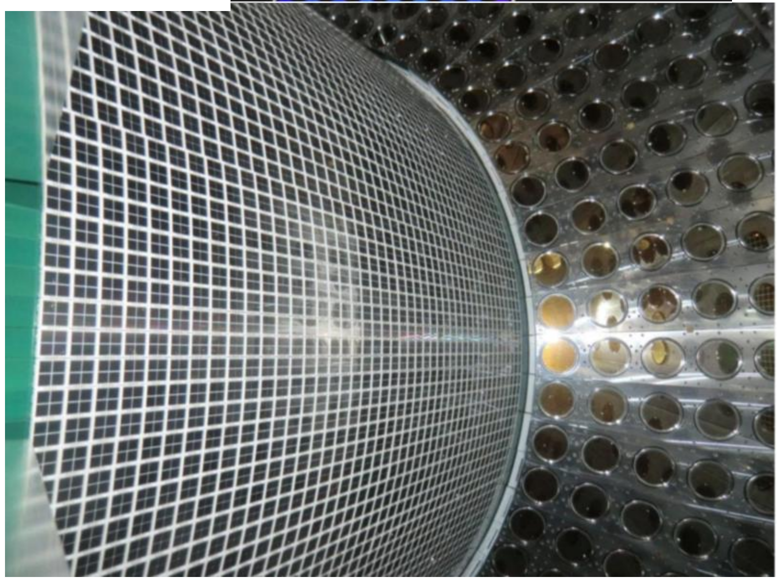

Kinematic Core σ	MEG I	MEG II Goal
E_γ (%)	**2.4**	**1.1**
u_γ (z_γ) (mm)	**5**	**2.6**
v_γ ($R\varphi_\gamma$) (mm)	**5**	**2.2**
w_γ (R_γ) (mm)	**6**	**5**
t_γ (ps)	**60**	**60**

LXe Detector

- One of world's largest liquid Xe detector (800 L)
- Upgrade: inner face PMTs replaced by 4092 15x15mm^2 MPPCs (Multi-Pixel Photon Counters)
- Other 5 sides remain covered by PMT photon counters

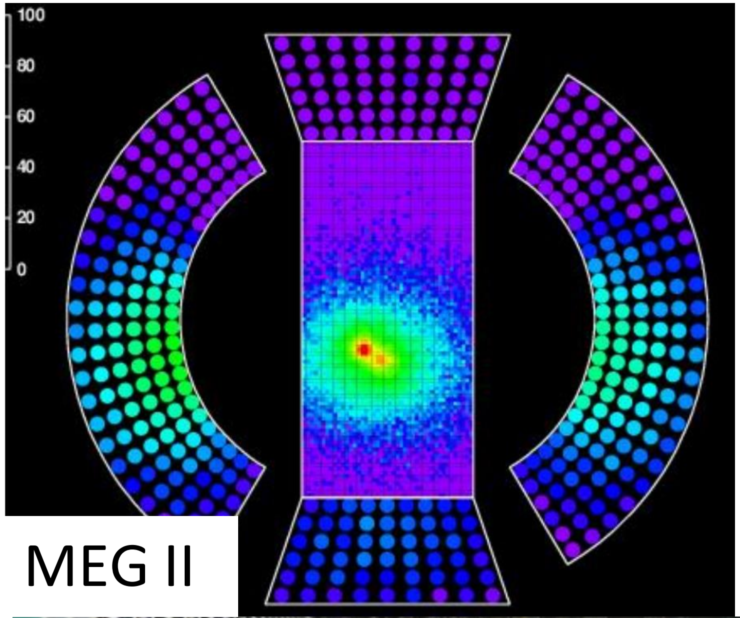

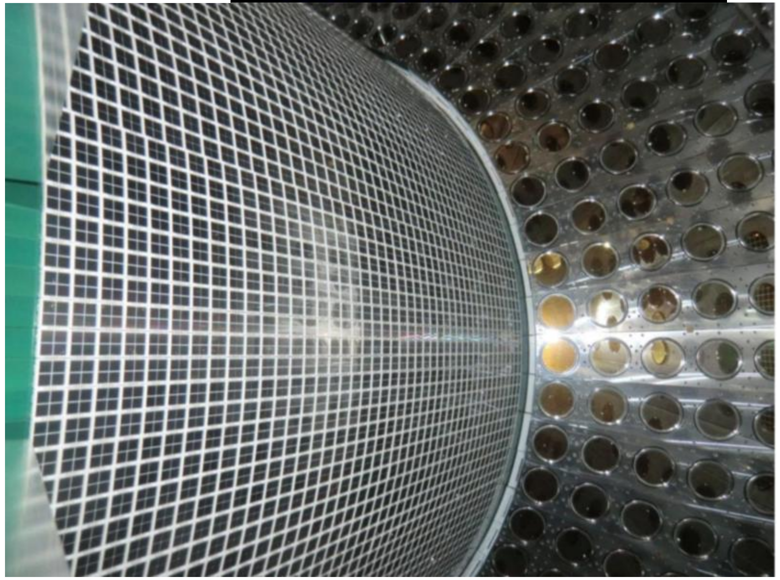

Kinematic Core σ	MEG I	MEG II Goal
E_γ (%)	**2.4**	**1.1**
u_γ (z_γ) (mm)	**5**	**2.6**
v_γ ($R\varphi_\gamma$) (mm)	**5**	**2.2**
w_γ (R_γ) (mm)	**6**	**5**
t_γ (ps)	**60**	**60**

Target Monitoring

- Motivation:
  Target 90 μm normal-displaced, φ_{e^+}=45°→
  e^+ path length error of 130 μm → 1 mrad φ_e error
- **One of the most dominant MEG I systematic errors**
- Relative target/CDCH coordinates:
  - Optical survey of the target/CDCH + pre-installation CT scan of target shape
  - 'Hole Analysis': image holes in made in target by lack of positrons originating from the hole position – incorrect target position results in reconstructed hole position varying with angle
  - Target motion measured by analyzing photographs taken periodically during data taking analysis

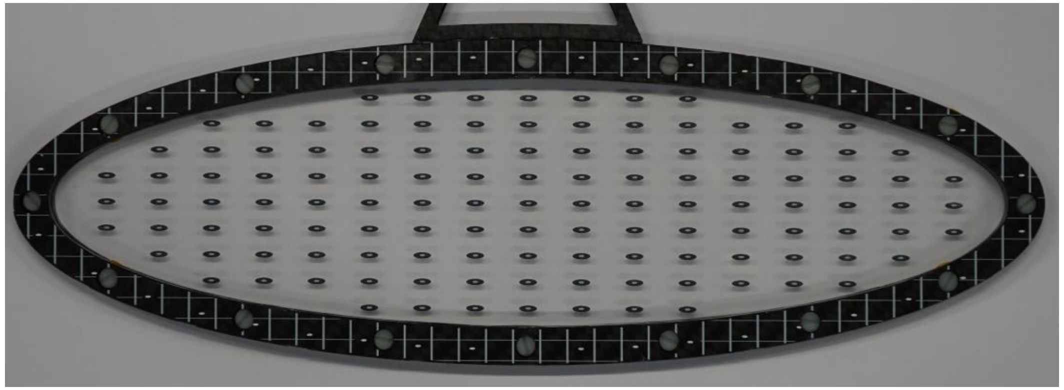

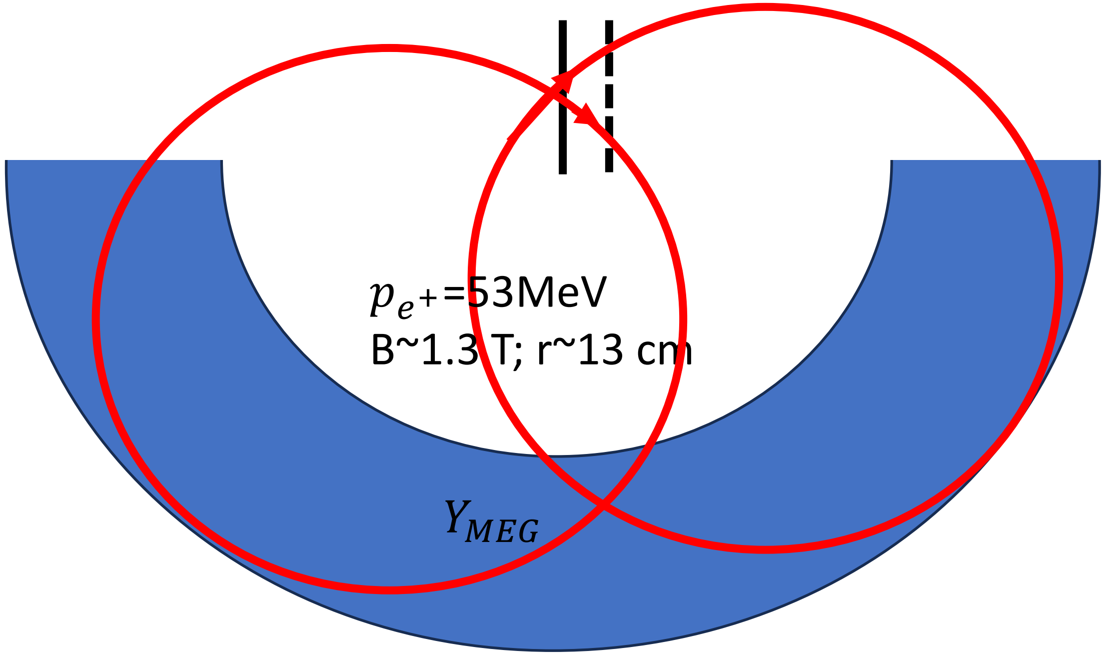

Target Monitoring

- Motivation:
  Target 90 μm normal-displaced, φ_{e^+}=45°→
  e^+ path length error of 130 μm → 1 mrad φ_e error
- **One of the most dominant MEG I systematic errors**
- Relative target/CDCH coordinates:
  - Optical survey of the target/CDCH + pre-installation CT scan of target shape
  - **'Hole Analysis': image holes in made in target by lack of positrons originating from the hole position – incorrect target position results in reconstructed hole position varying with angle**
  - Target motion measured by analyzing photographs taken periodically during data taking analysis

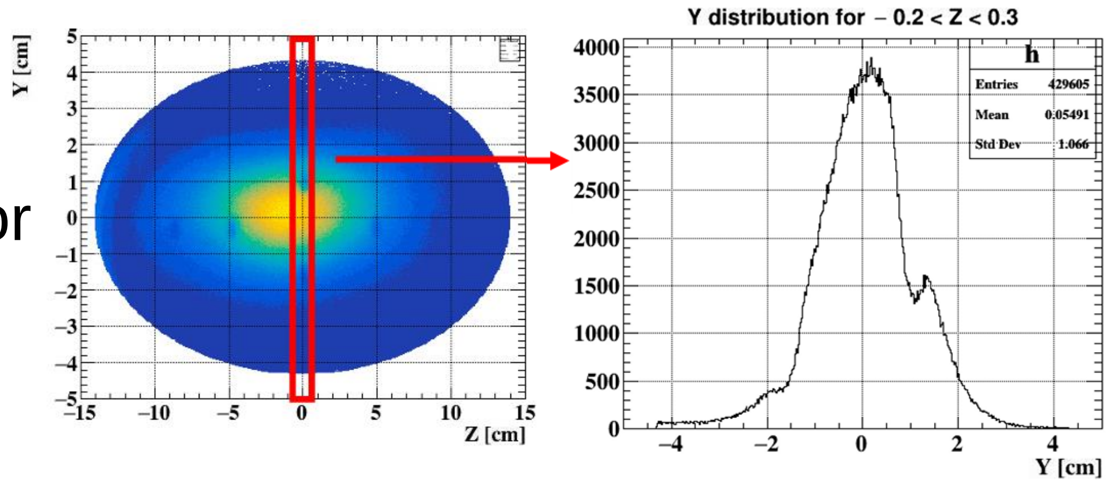

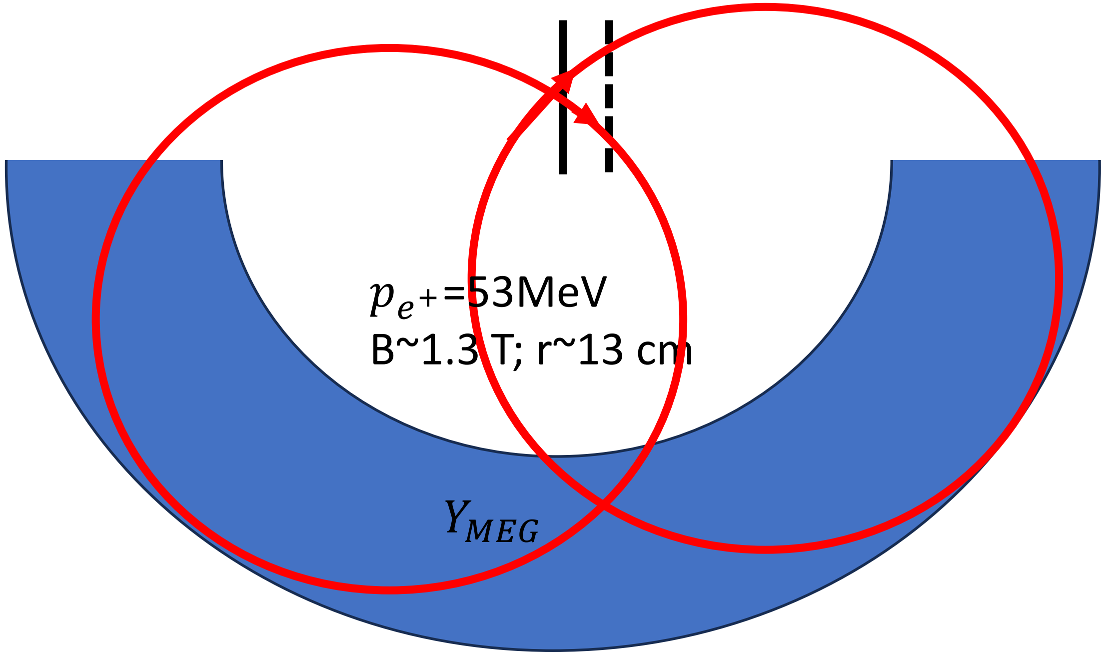

Target Monitoring

- Motivation:
  Target 90 μm normal-displaced, φ_{e^+}=45°→
  e^+ path length error of 130 μm → 1 mrad φ_e error
- **One of the most dominant MEG I systematic errors**
- Relative target/CDCH coordinates:
  - Optical survey of the target/CDCH + pre-installation CT scan of target shape
  - 'Hole Analysis': image holes in made in target by lack of positrons originating from the hole position – incorrect target position results in reconstructed hole position varying with angle
  - **Target motion measured by analyzing photographs taken periodically during data taking analysis**

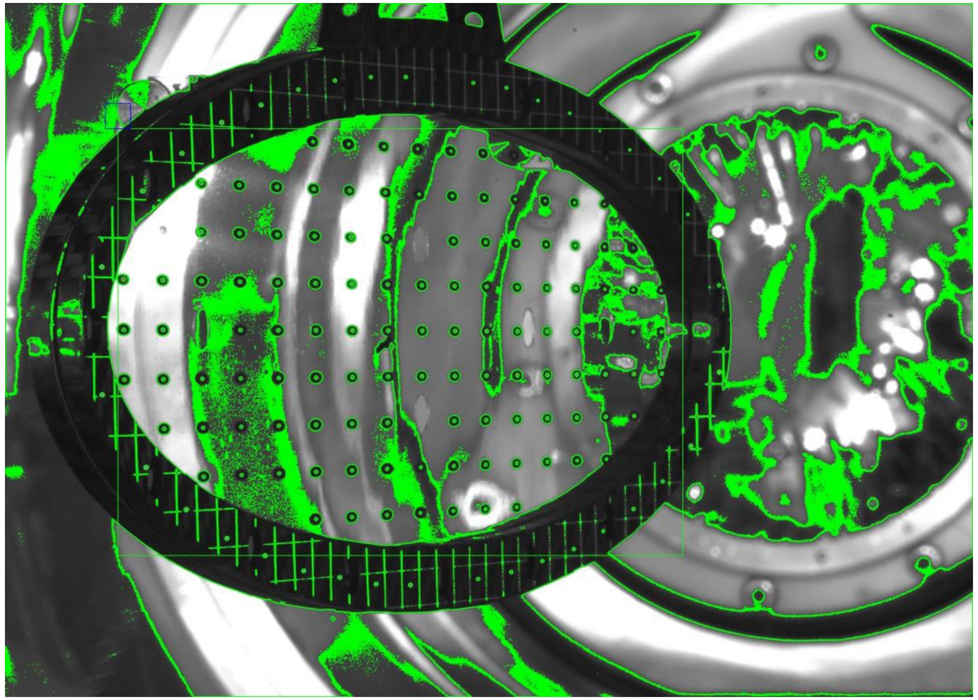

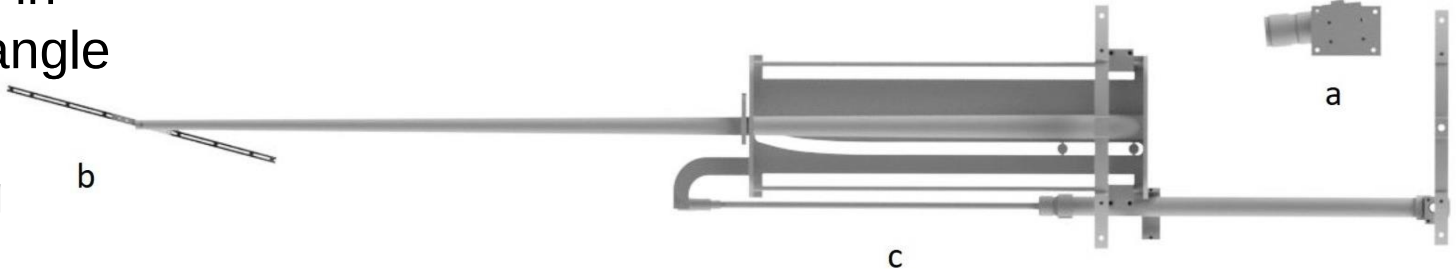

RDC Detector

- RDC eliminates a fraction of RMD accidental events using LXe/RDC matched γ/e^+
- Downstream of target only
- Remove events based on:
  - γ/e^+ relative timing (scintillator bars)
  - e^+ energy (LYSO crystal calorimeter)

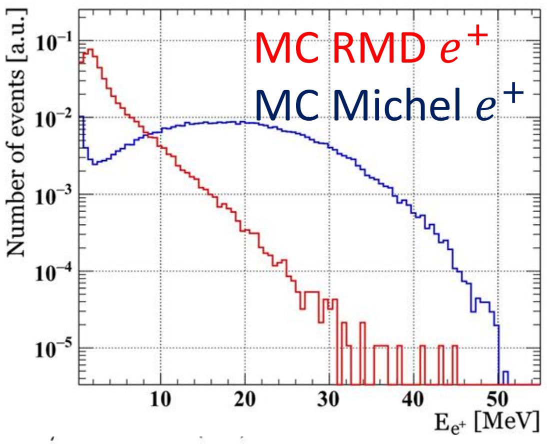

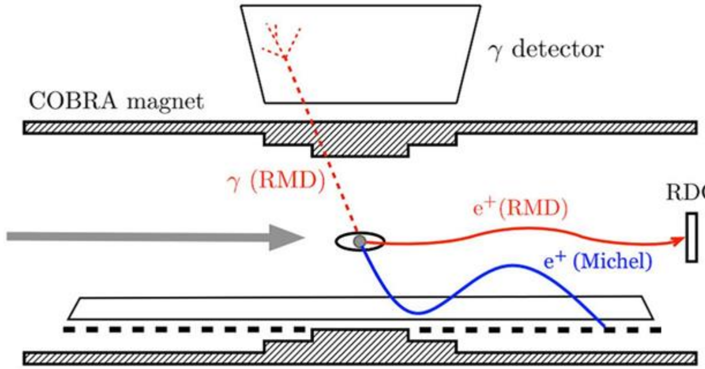

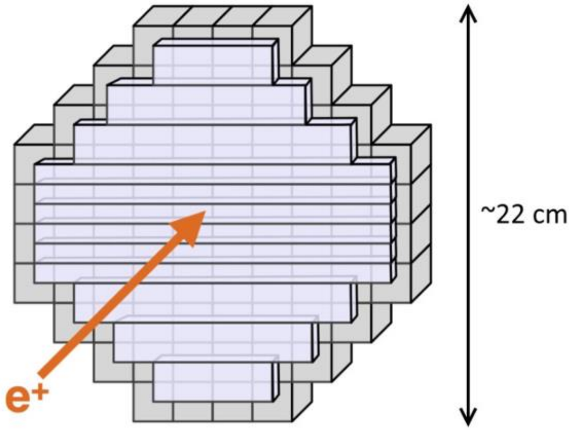

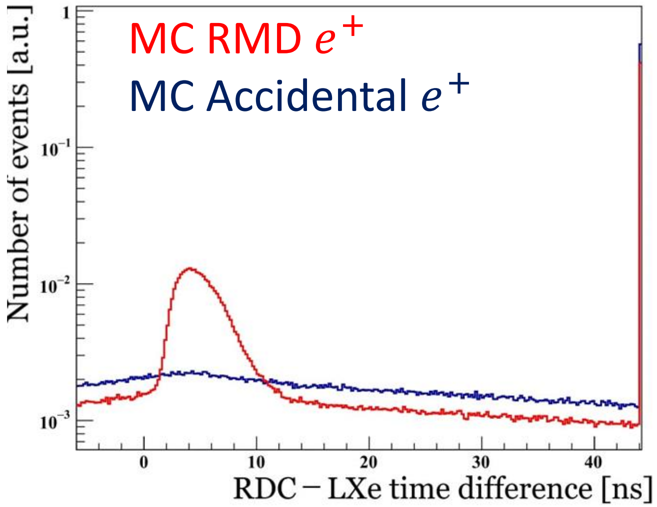

MEG Electronics

- All detectors use custom WaveDREAM (Waveform Domino READout Module) electronics boards
- O(10k) channels contain 1024 ‘sample-and-hold’ cells that sample and temporarily store detector signal (8x2 channels/board)
- After trigger, all charge is digitized via ADC
- Operated at a sampling frequency of 1.4 GHz

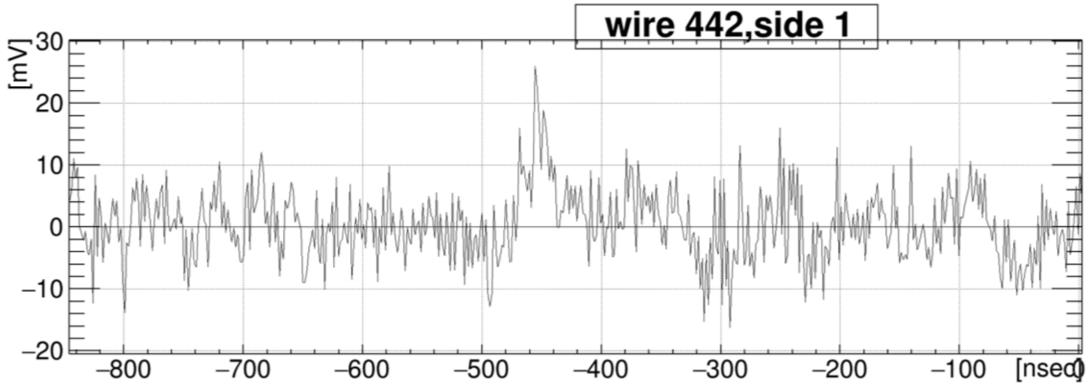

Ritt: https://doi.org/10.1016/j.nima.2003.11.059

MEG Trigger

- MEG Trigger Conditions:
  - LXe $E_\gamma > E_{\text{Threshold}}$ (40-45 MeV)
  - Time Match: pTC/LXe $|T_{e+/\gamma}| < 12.5$ ns
  - Spatial Match: pTC/LXe based on μ→eγ decays simulated in Geant4
- Trigger rate of ~ 12 Hz at 4×10^7 μ/s

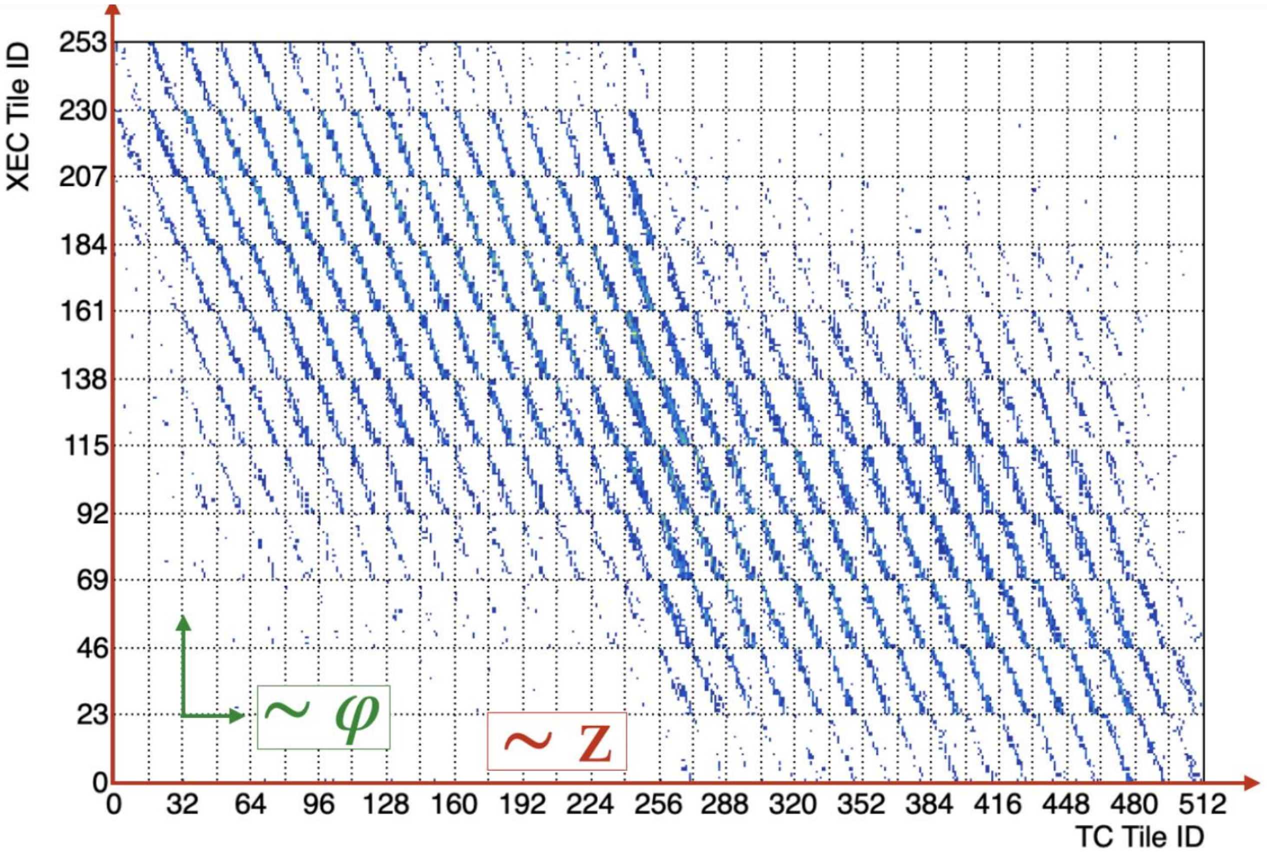

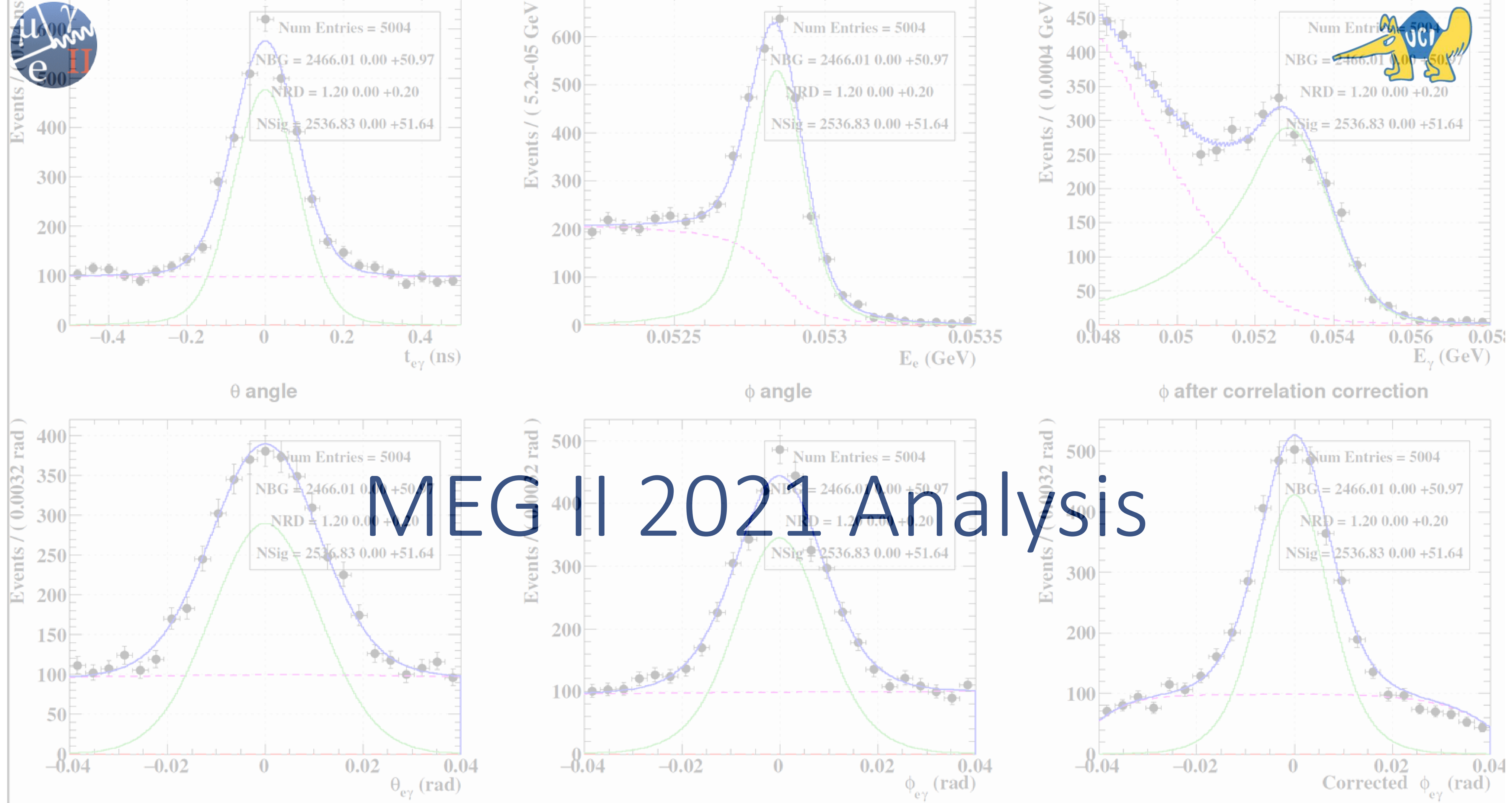

MEG II 2021 Analysis

Data Analysis

- **Optimizing resolutions/efficiency is critical to achieve the optimal sensitivity and ultimately detect μ→eγ**
- Much of the analysis work over the last couple years focused on noise suppression, calibrations, and alignment algorithms that were critical to improve resolutions and efficiency in the 2021 dataset
- Data Analysis:
  - **Positron analysis:**
    CDCH+SPX waveform data → e^+ kinematics
  - Photon Analysis:
    MPPC+PMT waveform data → γ kinematics
  - Target analysis: tracking target position, orientation, shape
  - RDC analysis: matching low momentum e^+ with LXe γ

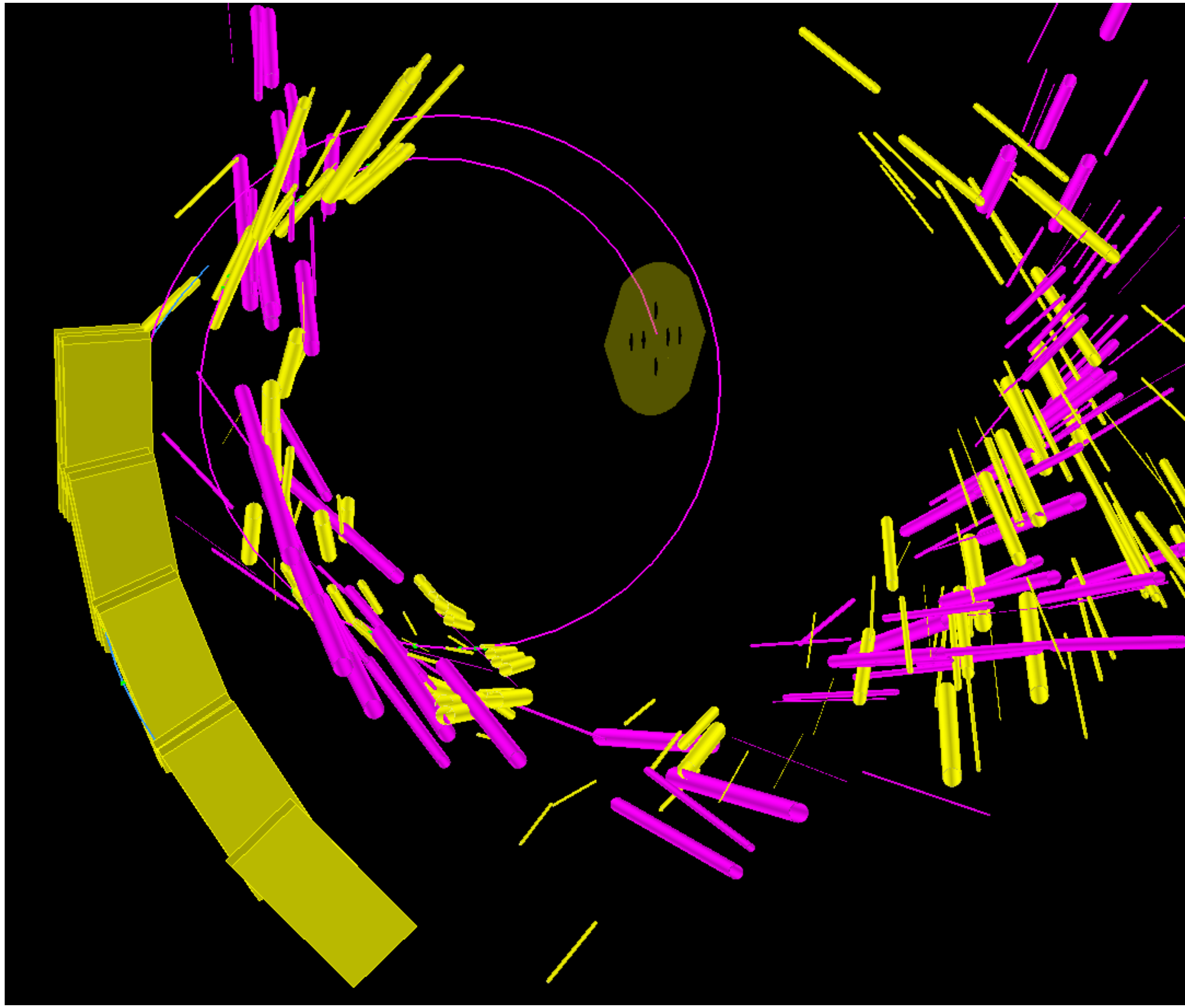

Positron Analysis

- Multi-step procedure to convert the CDCH+SPX digital waveforms into positron tracks
- Examples calibrations/alignments (bolded discussed):
  - Noise suppression
  - **CDCH wire-to-wire alignment**
  - **CDCH drift cell time-distance relationship**
  - CDCH+SPX time calibrations
  - Relative CDCH/SPX detector timing
  - Magnetic field calculation/measurement

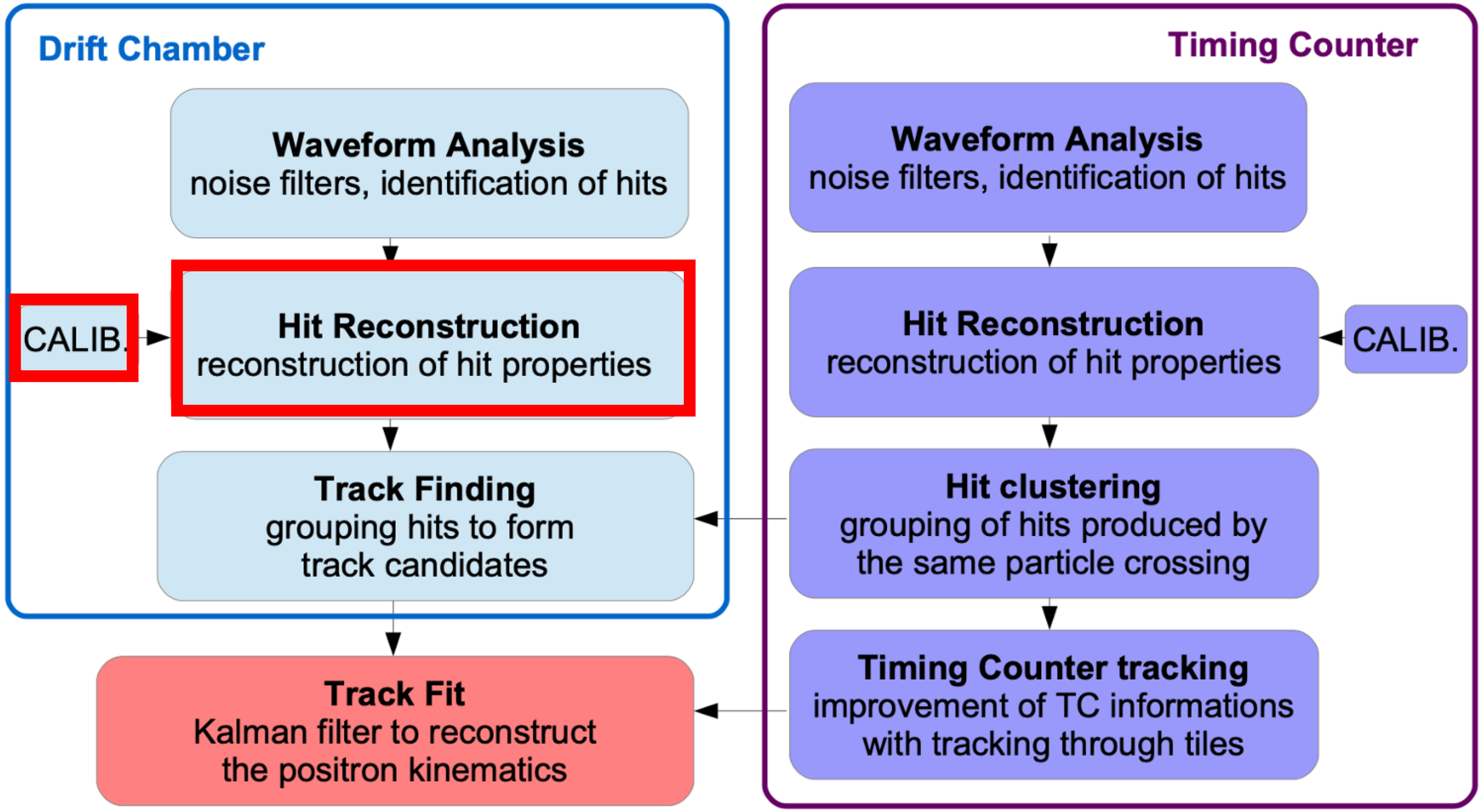

CDCH Waveform Analysis: Track Measurements

- Primary CDCH measurement is the track's distance of closest approach (DOCA) to a wire
- Analysis results in measured hit time. Combine with track T0 (from pTC), yields a drift time
- **Requires time-distance relationship to estimate the hit DOCA.** Conventionally calculated by Garfield
- Replaced by convolutional neural network (CNN) approach offers a data-driven approach by training on tracks in MEG data
- Improves DOCA resolution, reduces DOCA bias produced by ionization statistics, and improves kinematic resolutions

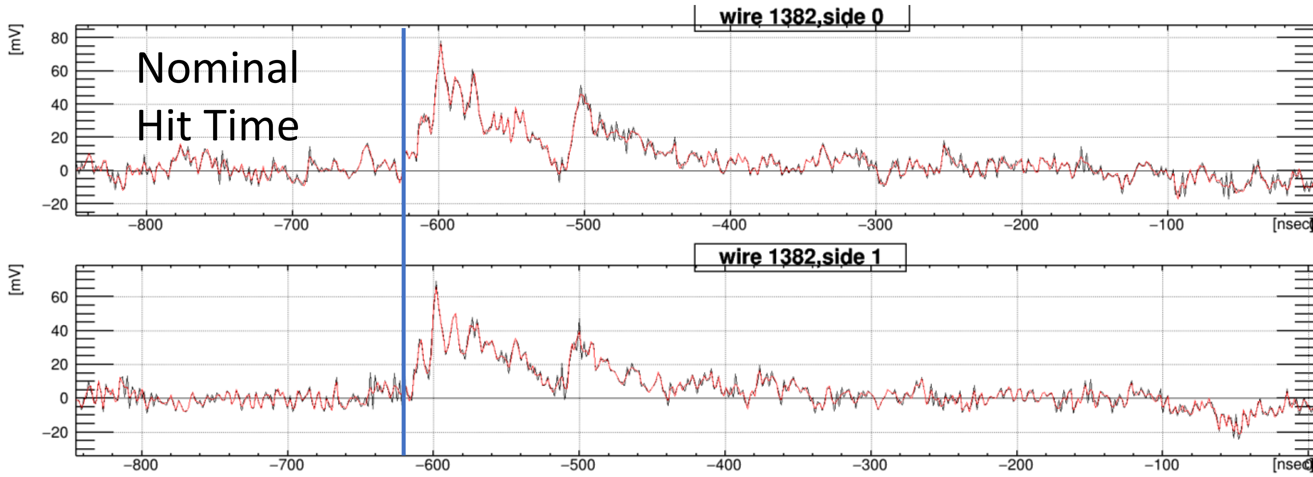

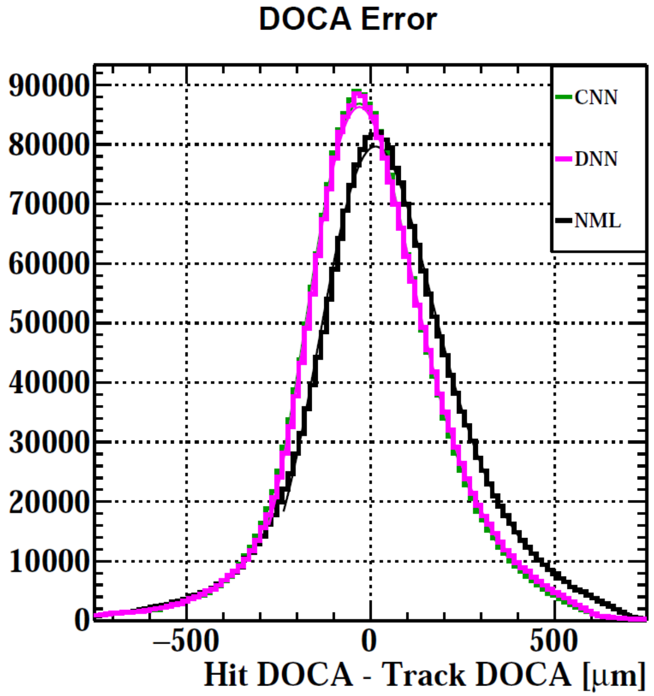

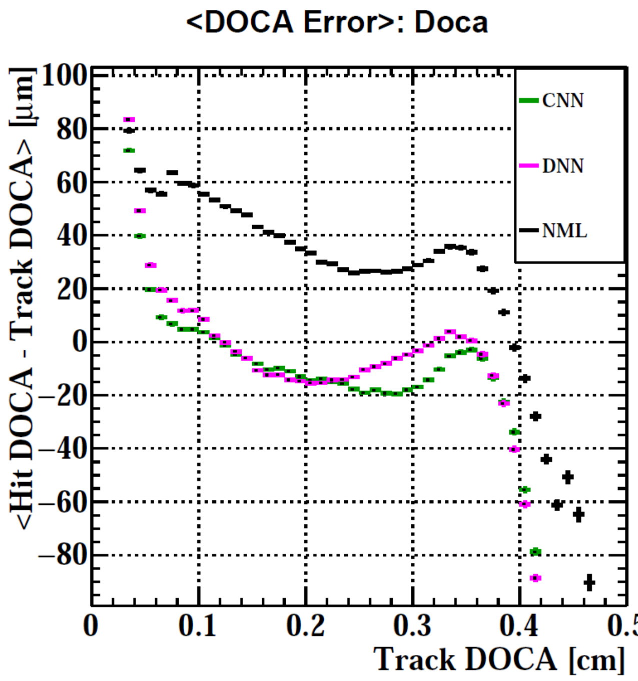

CDCH Wire Alignment

- Align the wires by calculating residuals as a function of position along the wire axis
- Iteratively correct the wire by applying translations, rotations, and a wire sagitta (electrostatic)
- Improves kinematic resolutions and biases in the kinematic resolutions

Survey Alignment

Average Y Error for Layer 4 Wires [μm]

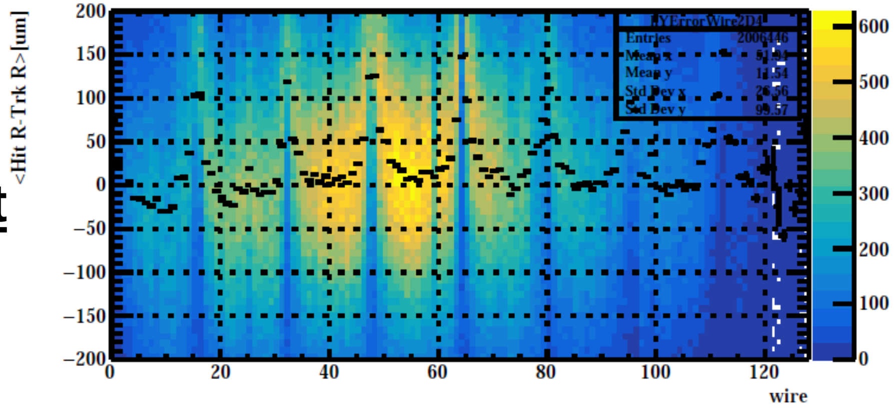

X Error on Wire 401[μm]

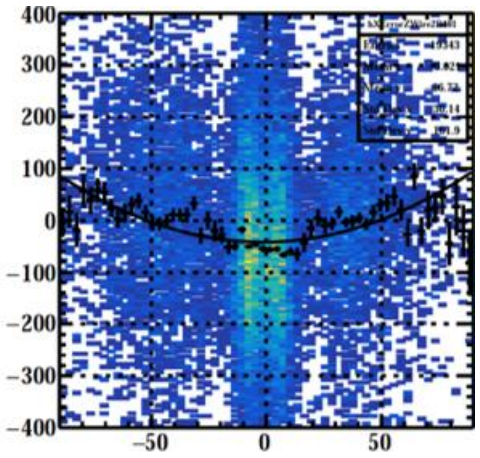

Axial Coordinate [cm]

Track-Based Alignment

Average Y Error for Layer 4 Wires [μm]

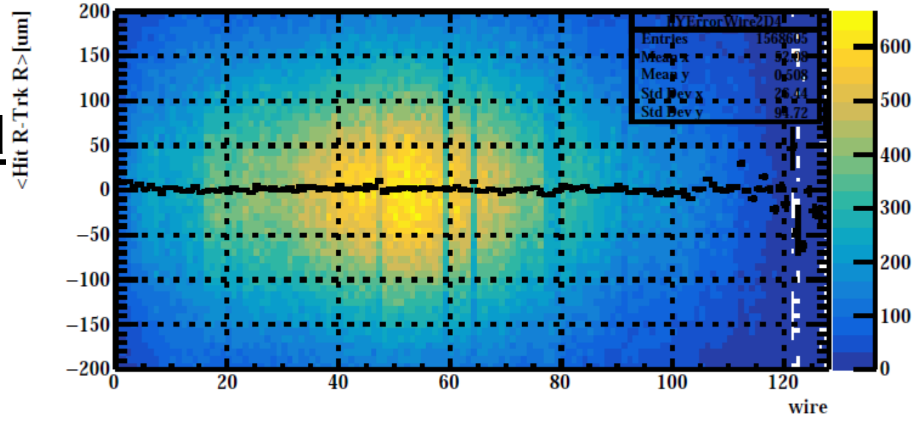

X Error on Wire 401[μm]

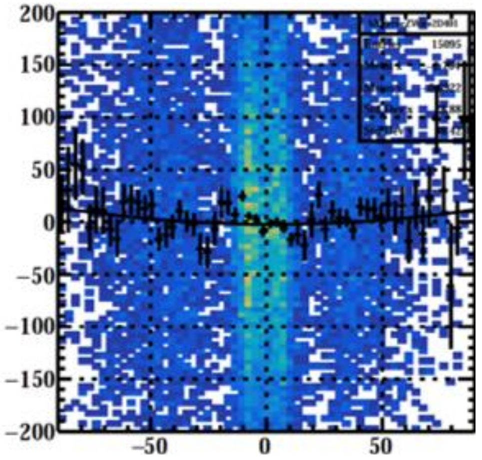

Axial Coordinate [cm]

- Goal: detect the $\mu^+ \to e^+ \gamma$ signal or calculate an upper-limit on BR of $\mu^+ \to e^+ \gamma$ using $E_\gamma, E_e, \varphi_{e\gamma}, \theta_{e\gamma}, t_{e\gamma} + (t_{RDC-LXE}, E_{RDC})$
- Two **blind** physics analyses discussed in next few slides:
  - Cut and count analysis (2 separate analyses)
  - Maximum likelihood analysis (2 separate analyses)
- Common requirements:
  - **Calibrations, alignments, noise suppression**
  - **Positron/photon selection**
  - **Kinematic resolution estimates**
  - Correlations between kinematics
  - Both opt to include event-by-event information
  - **Estimates of background rates/distributions**

NN Track Selection Trained Directly On Data To Remove Mismeasured Tracks

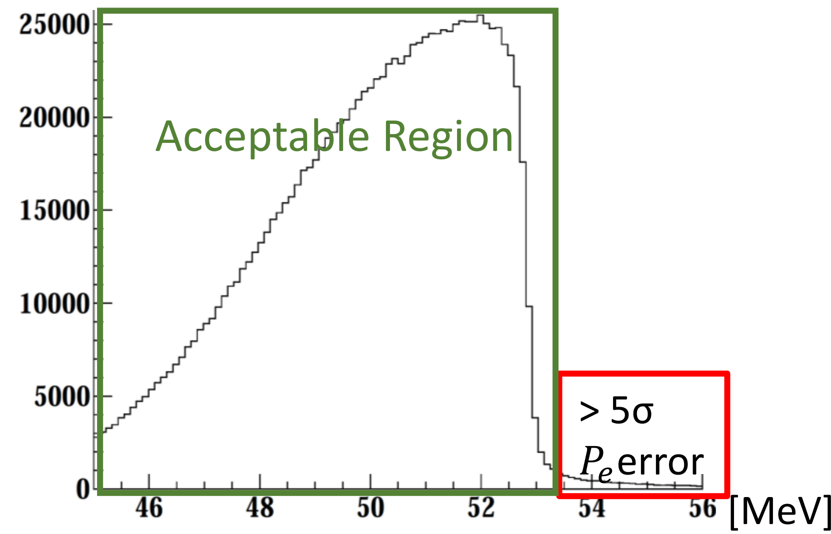

NN Accuracy with Varying Inputs

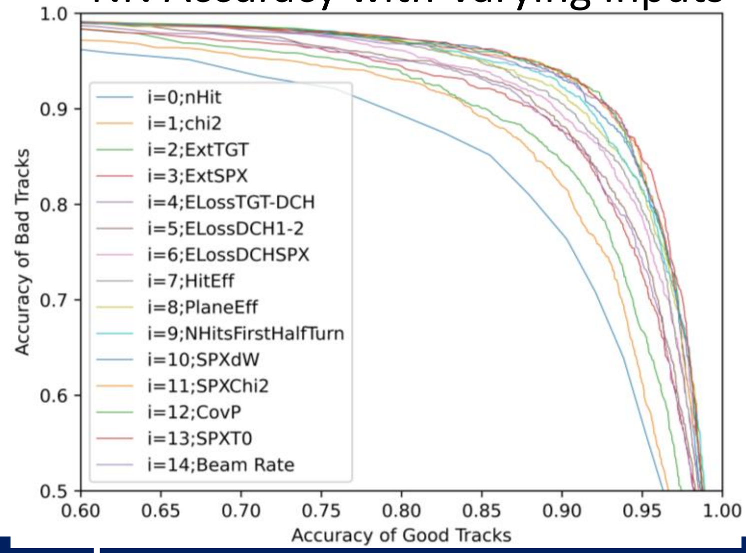

Resolution Estimates

- Will highlight some of the data-driven kinematic resolution estimate approaches for the CDCH, pTC, and LXe detectors
- Optimal resolutions are required to suppress the background

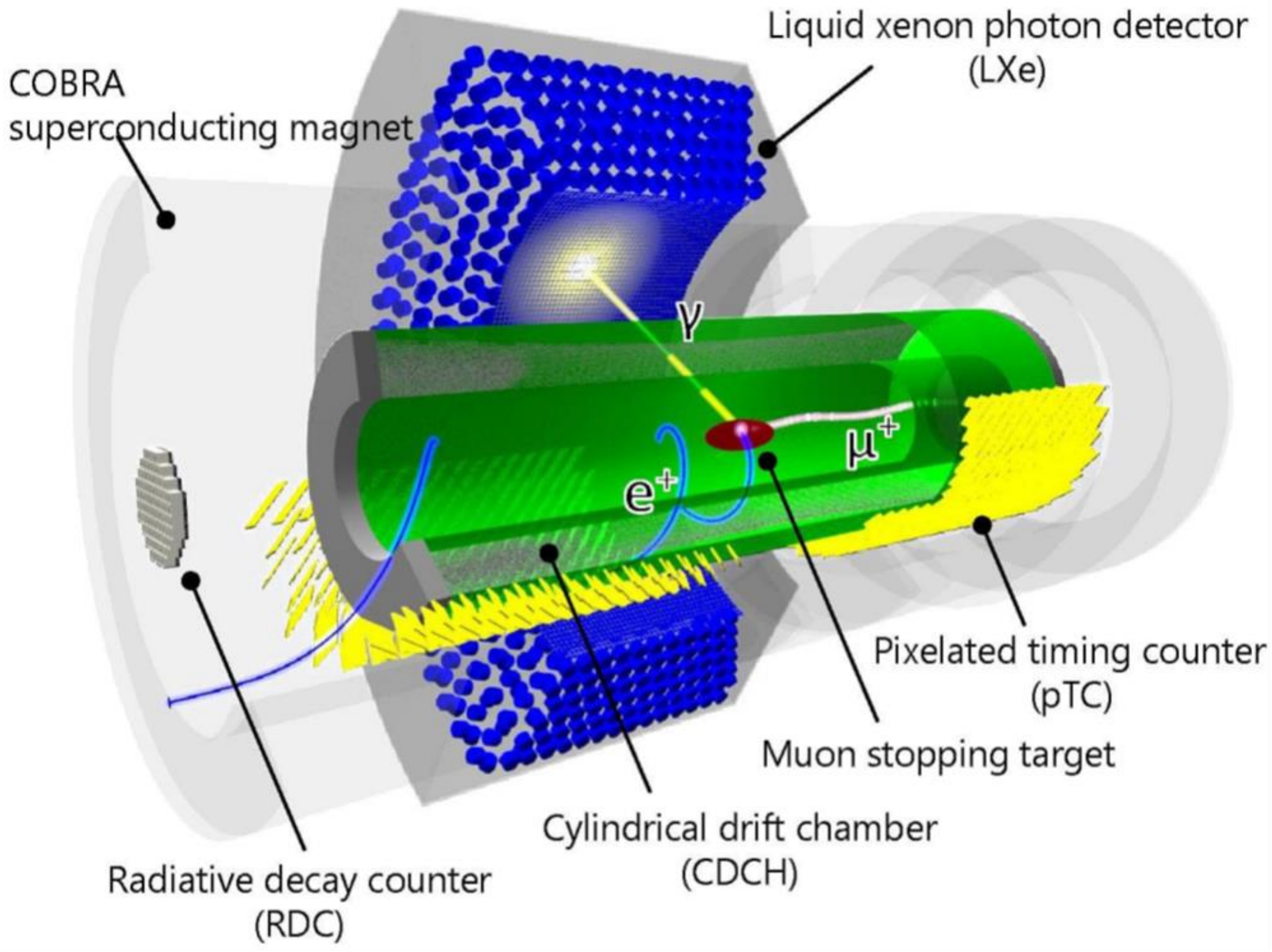

Positron Resolution

- Data-driven e^+ kinematic resolution estimate compares two independently measured/fit turns on a single e^+ track: double turn analysis
- Compare kinematics at a common plane between the turns

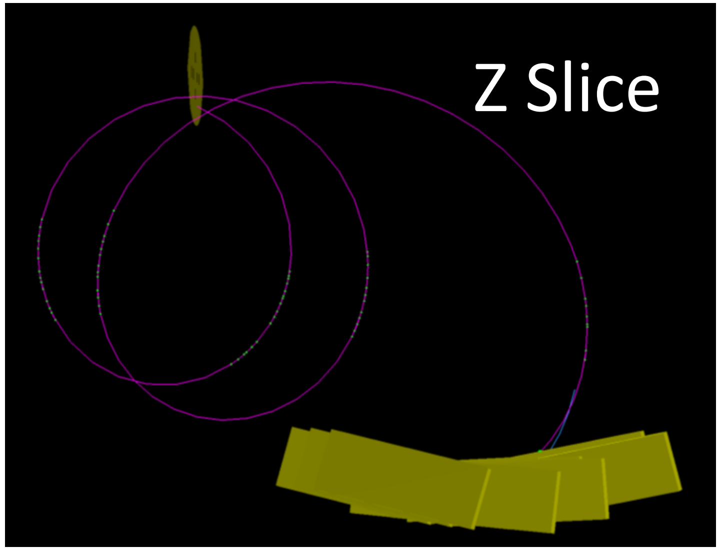

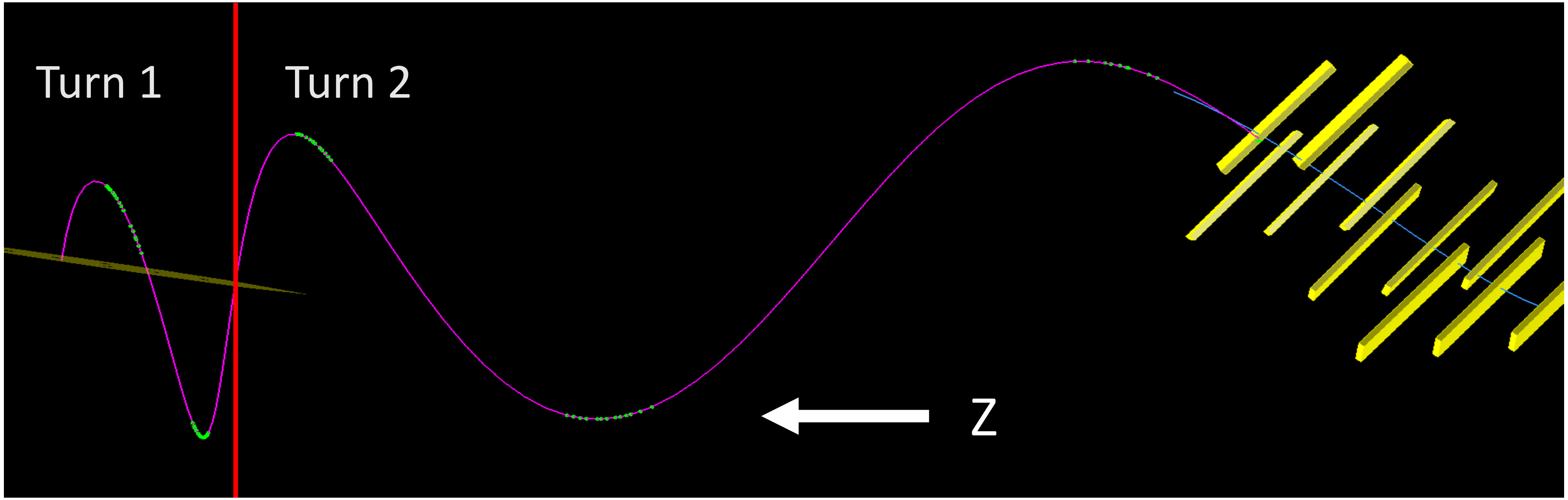

Double Turn Analysis

- Turn kinematic comparison at target plane
- $\sigma^2_{\Delta A} = \sigma^2_{Turn\ 2} + \sigma^2_{Turn\ 1}$
- Fit to convolution of two double gaussians
- Yields quality estimate of the core/tail resolution that only requires minor MC corrections

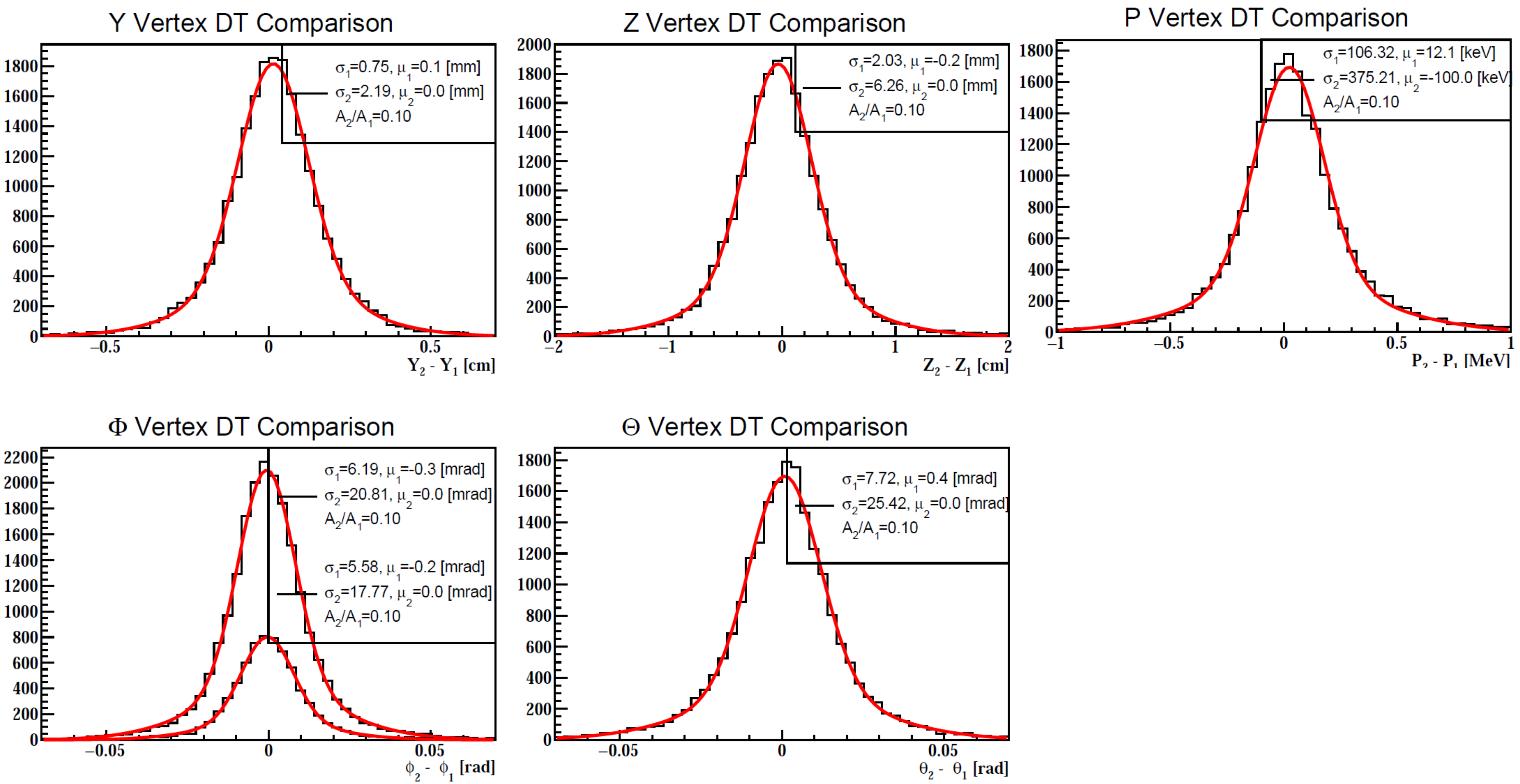

ϕ_{e+} estimated at plane perpendicular to track, smaller ϕ_{e+} is at $|\phi_{e+}| < 0.2$ rad

Double Turn Analysis

- Resolutions measured with double turn analysis (DT) are all improved with respect to MEG I and close to goal
- Improving single hit resolution, magnetic field map, etc. aim to achieve the MEG II goal resolutions

$3 \cdot 10^7 \mu/s$

Kinematic Resolution	MEG I Core σ	MEG II Goal Core σ	MEG II 2021 DT Core σ
p_{e_+} (keV)	380	130**	**97**
θ_{e+} / φ_{e+}*(mrad)	9.4/8.7	5.3/3.7	**7.2/4.1**
z_{e+} / y_{e+} (mm)	2.4/1.2	1.6/0.7	**2.0/0.7**

*φ_{e+} estimated at plane perpendicular to track, includes correlations
**based on early CDCH track fitting algorithms

XEC Resolutions

- CEX Reaction:
  - $\pi^- \, p \rightarrow \pi^0 \, n;\ \pi^0 \rightarrow \gamma\ \gamma$
  - $E_\gamma = 0.5 m_{\pi_0} \gamma (1 \pm \beta \cos \theta_{rest})$
  - $\theta_{rest} = 0; \beta \sim 0.2; E_\gamma = 55/83$ MeV
- Separate detector (BGO) selects back-to-back γ pair ($dt_{BGO-LXe}$, E_{BGO}, Opening angle > 170 deg)
- CEX reaction used to
  - Calibrate E_γ, t_γ
  - Estimate σ_{E_γ}, σ_{t_γ}
- Ongoing work to calibrate LXe to achieve MEG II goal resolutions (E_γ)

LXe CEX Setup

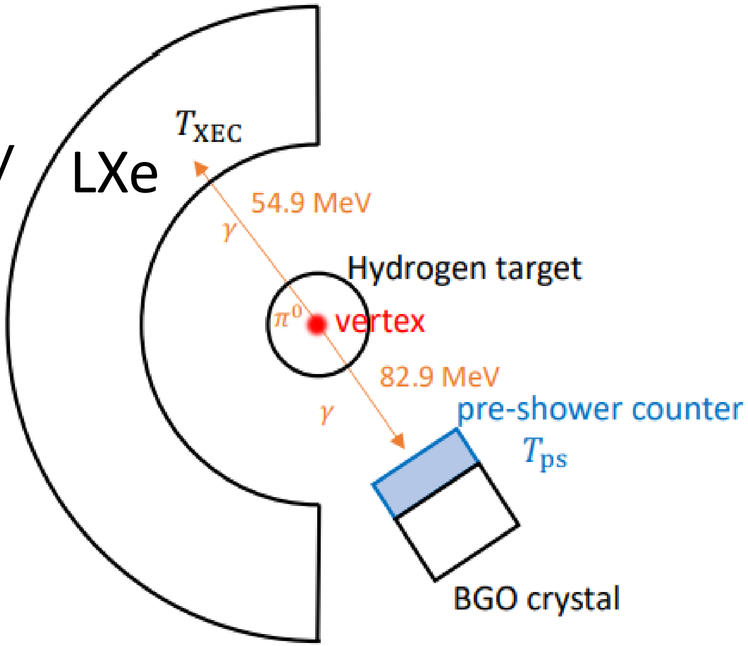

LXe CEX Energy Distribution with Varying Depth (w)

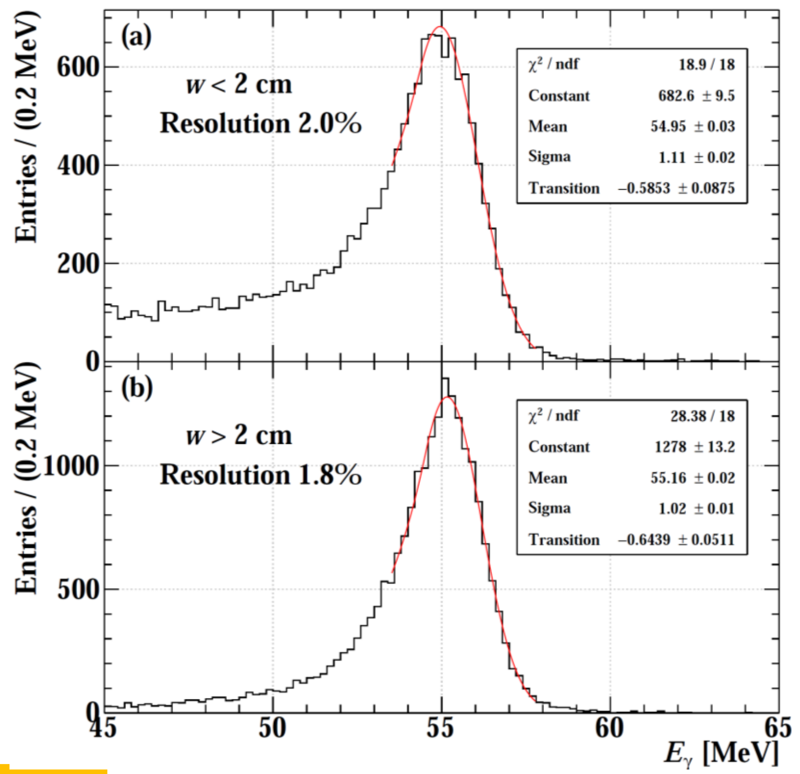

Kinematic Resolution	MEG I	MEG II Goal	MEG II 2021
E_γ (%)	2.4	1.1	**1.9**
t_γ (ps)	60	60	70

2021 RMD Timing Peak

- Use non-accidental RMD e^+/γ pairs at standard beam intensity to estimate $\sigma_{t_{e^+\gamma}}$
- Direct measurement of $\sigma_{t_{e^+\gamma}}$
- Signal e^+ contains ~9 N_{TC}. For events with 9 N_{TC}, $\sigma_{t_{e^+\gamma}}$ ~78 ps
- Comparable to MEG II goal of 84 ps

RMD $t_{e_+\gamma}$ with TC per-event Errors

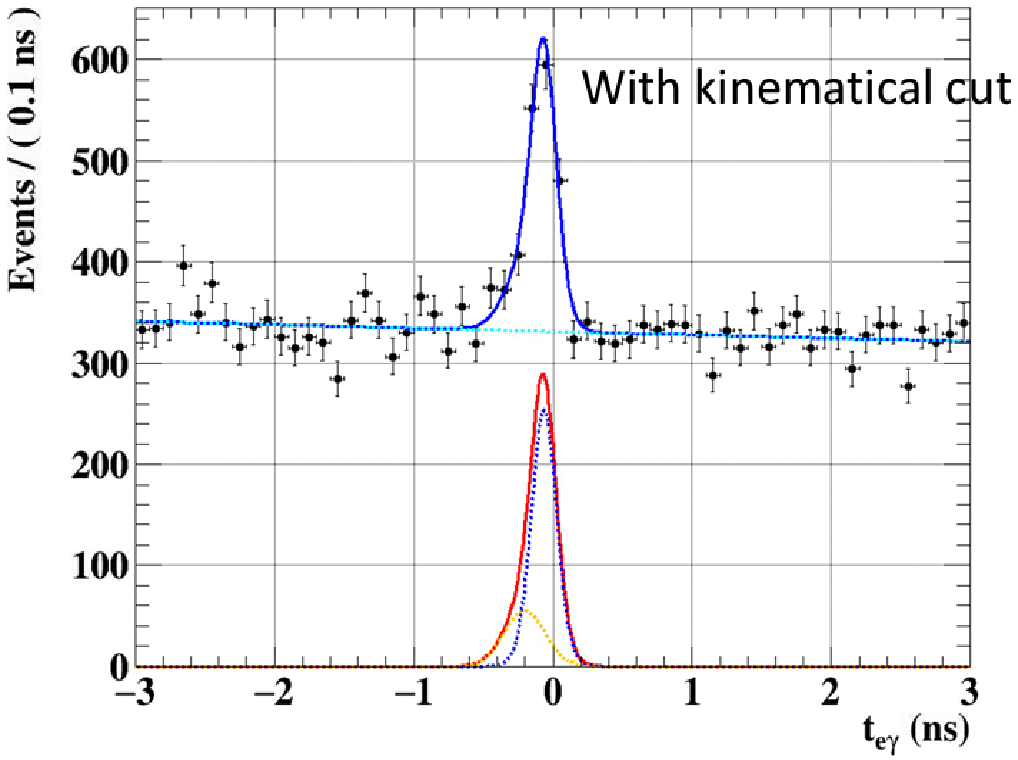

Physics Analysis Tools: Background

- Tools to estimate background rates/distributions in the signal region
- Time sideband:
  - Signal region offset in $t_{e^+\gamma}$
  - Estimate N_{ACC} in signal region
  - Calculate distribution of accidentals (e.g. E_γ, p_e) expected in the signal region
- Energy sideband:
  - Signal region shifted to lower E_γ
  - Estimate N_{RMD} in signal region; found to be completely negligible
- Toy MC:
  - Use resolutions and sideband results to generate many toy MC "experiments"
  - Toy MC experiments contain expected accidental distributions: used to calculate the upper-limit in the absence of signal

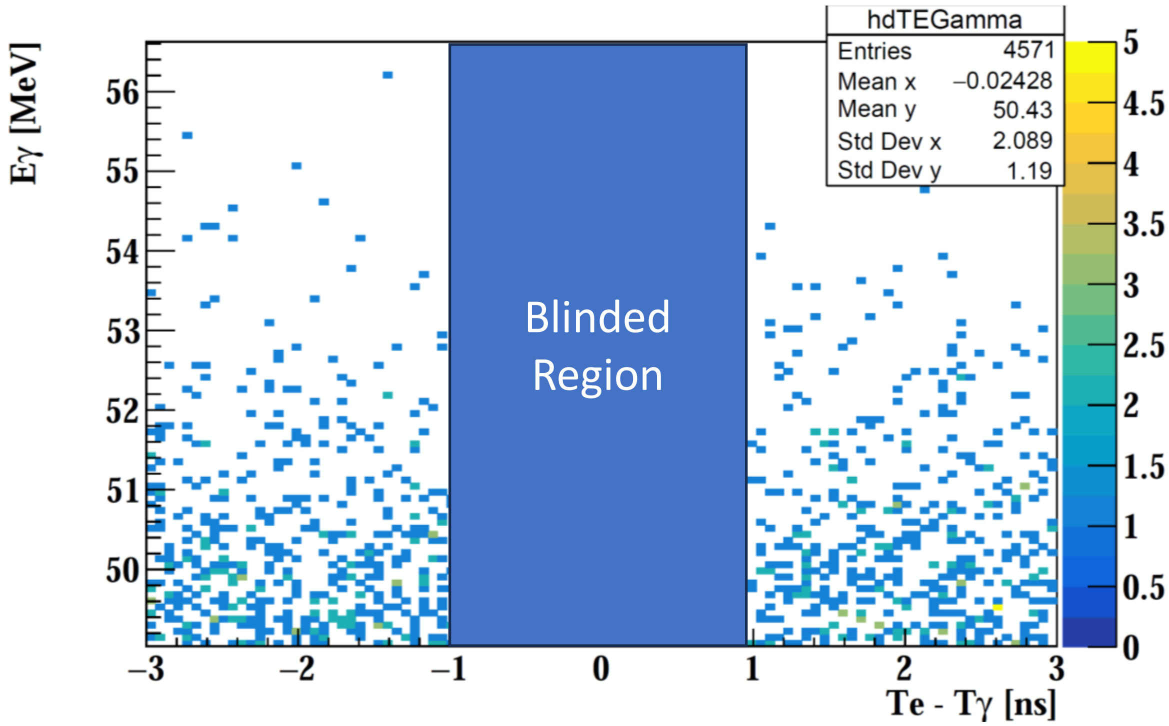

Probability Density Functions

- Using kinematic resolutions and sideband information we build signal and accidentals PDFs (graphic shows equal weighting)

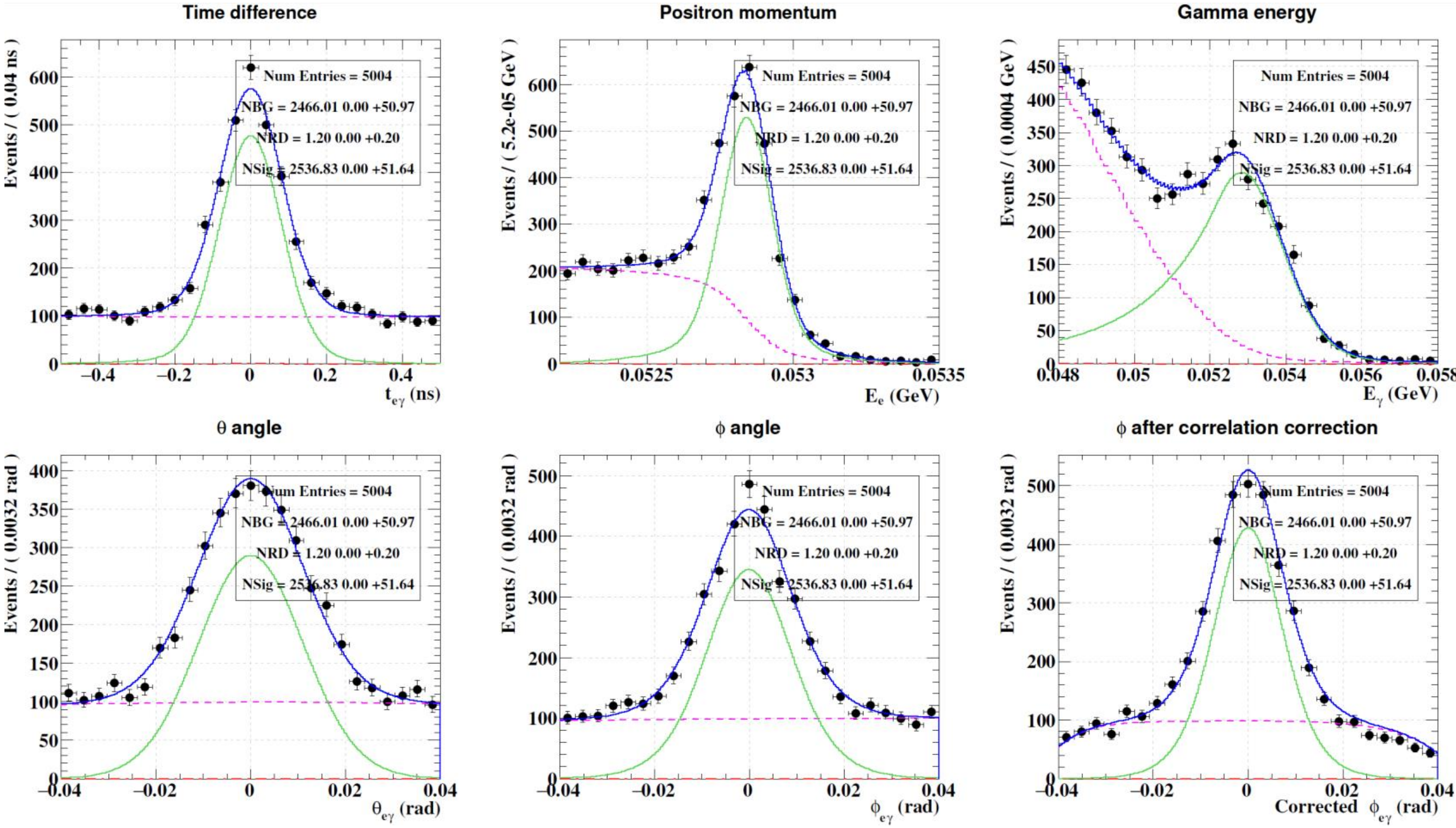

Maximum Likelihood Analysis

- Maximum likelihood analysis (MLA) uses the signal/background PDFs to fit for $N_{SIG}, N_{ACC}, N_{RMD}, X_{TGT}$
- Extended Likelihood function:

$$L(\vec{\theta}) = \frac{e^{-N} N^n}{n!} \prod_{i=1}^{n} p(\vec{x}_i; \vec{\theta})$$

$$L(N_{\mathrm{sig}}, N_{\mathrm{RMD}}, N_{\mathrm{Acc}}, X_{\mathrm{TGT}}) := \exp\left(-\frac{(X_{\mathrm{TGT}})^2}{2\sigma_{\mathrm{TGT}}^2}\right) \times \exp\left(-\frac{(N_{\mathrm{RMD}} - \langle N_{\mathrm{RMD}}\rangle)^2}{2\sigma_{\mathrm{RMD}}^2}\right) \times \exp\left(-\frac{(N_{\mathrm{Acc}} - \langle N_{\mathrm{Acc}}\rangle)^2}{2\sigma_{\mathrm{Acc}}^2}\right) \times \frac{e^{-(N_{\mathrm{sig}}+N_{\mathrm{RMD}}+N_{\mathrm{Acc}})}}{N_{\mathrm{obs}}!} \prod_{i=1}^{N_{\mathrm{obs}}} \left(N_{\mathrm{sig}} S(\vec{x}_i | X_{\mathrm{TGT}}, \vec{q}_i) + N_{\mathrm{RMD}} R(\vec{x}_i|\vec{q}_i) + N_{\mathrm{Acc}} A(\vec{x}_i|\vec{q}_i)\right)$$

Nuisance Parameters

- Applying the MLA to toy MC in the absence of signal, we estimate a median upper-limit on N_{SIG} of 2.21 at the 90% CL

Toy MC in the absence of signal

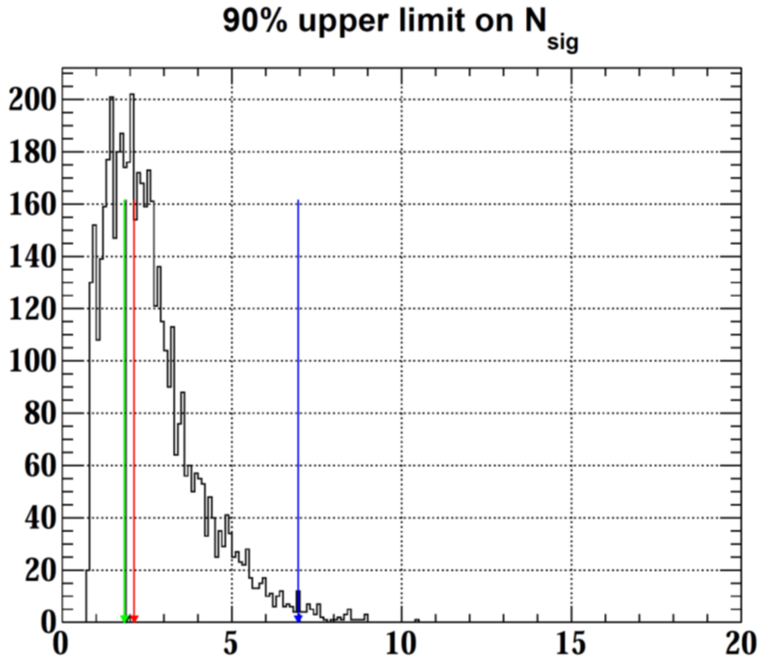

Cut and Count Analysis

- Cut and count analysis (CCA): define a signal region and count the number of events inside (N_{SIG}). No RDC used
- The analysis region is defined by a hyperradius ($r_H < 3.45$):

$$r_H = \sqrt{\left(\frac{t_{e\gamma}}{\sigma_{t_{e\gamma}}}\right)^2 + \left(\frac{\phi_{e\gamma}}{\sigma_{\phi_{e\gamma}}}\right)^2 + \left(\frac{\theta_{e\gamma}}{\sigma_{\theta_{e\gamma}}}\right)^2 + \left(\frac{(\frac{m_\mu}{2} - \alpha) - p_e}{\sigma_{p_e}}\right)^2 + \left(\frac{(\frac{m_\mu}{2} - \beta) - E_\gamma}{\sigma_{E_\gamma}}\right)^2}$$

- Calculate <N_{ACC}> in signal region using time sidebands and toy MC: <N_{ACC}> =0.61 events
- The median/mode toy MC experiment results in zero events
- Using the Feldman Cousins approach, this null signal would result in an UL on N of 1.8 at the 90% CL, but a lower signal efficiency (<UL> of 2.95 at the 90% CL)

N_{ACC} in Toy MC in the absence of signal

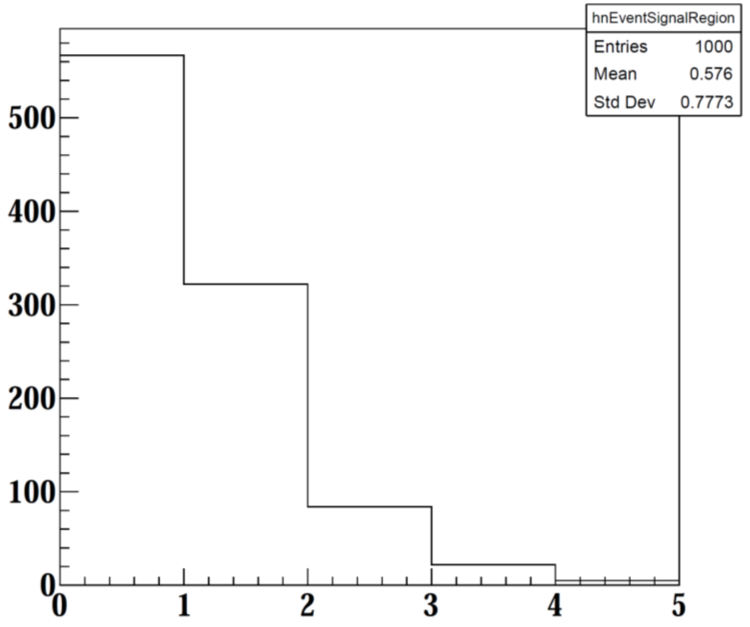

Normalization

- In either physics analysis, to convert the upper-limit on N into a branching fraction of $\mu^+ \rightarrow e^+\gamma$, we require the number of μ^+ observed in our dataset, N_μ
- *Single event sensitivity is the branching fraction that would result in 1 signal event in the dataset i.e., $1/N_\mu$
- Measure N_μ using two techniques:
  - Measure the number of positrons reconstructed in a trigger requiring only an SPX hit:

$$N_\mu = N_{e\nu\overline{\nu}} \cdot P_{e\nu\overline{\nu}} \cdot \frac{1}{f(e\nu\overline{\nu},*)} \cdot \frac{\epsilon_{TRG}^{e\gamma}}{\epsilon_{TRG}^{e\nu\overline{\nu}}} \cdot \frac{\epsilon_e^{e\gamma}}{\epsilon_e^{e\nu\overline{\nu}}} \cdot A_{e\gamma} \cdot \epsilon_\gamma^{e\gamma} \cdot \epsilon_{SEL}^{e\gamma}$$

  - Measure the number of RMD events in the physics trigger sample (45 < E_γ 48 MeV):

$$N_\mu = N_{e\nu\overline{\nu}\gamma} \cdot \frac{1}{B(e\nu\overline{\nu}\gamma,*)} \cdot \frac{\epsilon_{TRG}^{e\gamma}}{\epsilon_{TRG}^{e\nu\overline{\nu}\gamma}} \cdot \frac{\epsilon_e^{e\gamma}}{\epsilon_e^{e\nu\overline{\nu}\gamma}} \cdot \frac{\epsilon_\gamma^{e\gamma}}{\epsilon_\gamma^{e\nu\overline{\nu}\gamma}} \cdot \frac{\epsilon_{SEL}^{e\gamma}}{\epsilon_{SEL}^{e\nu\overline{\nu}\gamma}}$$

  - Both require acceptance and efficiency terms estimated from a variety of sources e.g. calibration data, alternate trigger data, Monte Carlo, etc.
- Normalization measurements agree within 2σ
- Normalization of MLA is $2.64 \cdot 10^{12}$, CCA is $1.98 \cdot 10^{12}$ due to a lower signal efficiency

Sensitivity From Toy MC

- ‘Sensitivity’ is median toy MC upper-limit in the absence of signal:
  upper-limit on N_{SIG} divided by the normalization, N_μ: $UL_{N_{SIG}} / N_\mu$
- This is the median upper-limit we expect to set in the absence of signal
- MEG II 2021 dataset sensitivity approaches that of MEG I
- Projects to reach its goal sensitivity by end of MEG II lifetime

Dataset	Sensitivity (10^{-13})	Single Event Sensitivity (10^{-13})
MEG I Sensitivity	5.3	0.58
MEG II 2021 Sensitivity CCA	9.3	5.0
MEG II 2021 Sensitivity MLA	8.8	3.8

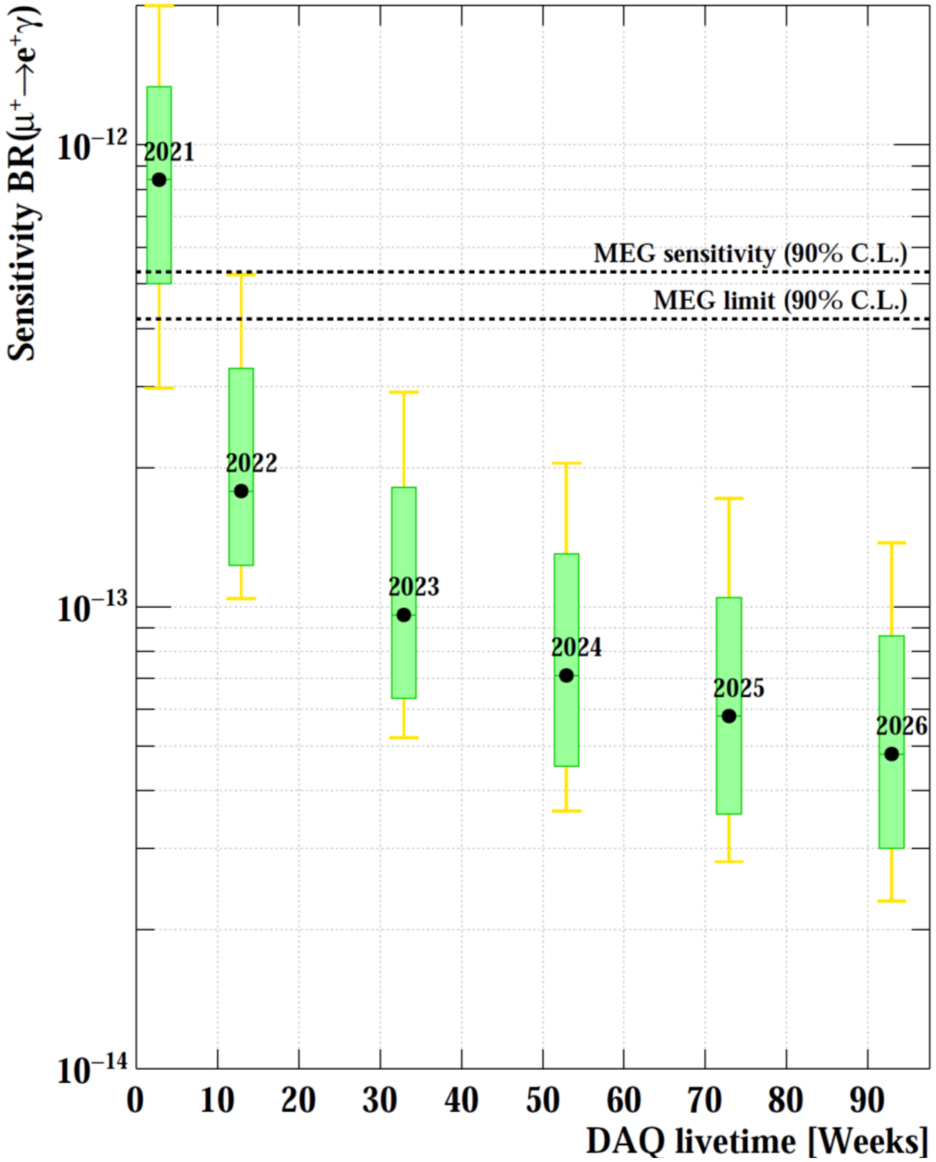

Signal Region

- The CCA resulted in a null signal therefore resulting in an upper-limit of $9.3*10^{-13}$
- The MLA resulted in an upper-limit on N_{SIG} of 1.98 i.e., an upper-limit of $7.5*10^{-13}$ NLL is comparable to that of toy MC
- Both results are in good agreement with the toy MC experiments (close to median)

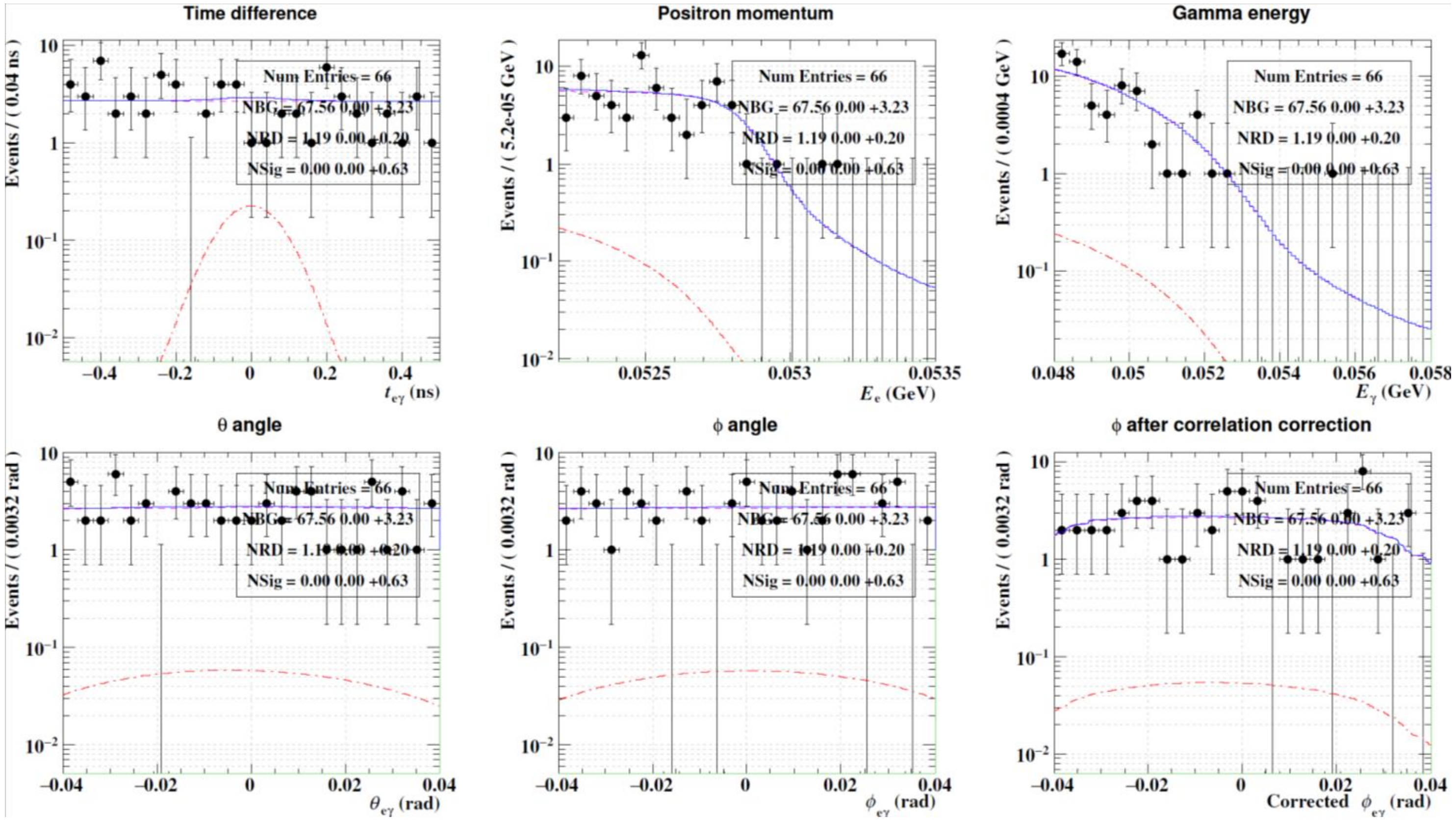

Signal Region

- The CCA resulted in a null signal therefore resulting in an upper-limit of 9.3*10^{-13}
- The MLA resulted in an upper-limit on N_{SIG} of 1.98 i.e., an upper-limit of 7.5*10^{-13} NLL is comparable to that of toy MC
- The top ranked events from the CCA are shown below. Good agreement between the top ranked MLA and CCA events

Run #	Event #	$\theta_{e\gamma}$ [mrad]	$\phi_{e\gamma}$ [mrad]	E_e [MeV]	E_γ [MeV]	$t_{e\gamma}$[ns]	r_H	MLA Rank
402458	22	1.3	3.4	52.69	49.51	0.14	4.2	2
401563	1286	-27.7	-2.2	52.97	51.95	-0.11	4.2	1
403059	2406	-13.3	-1.4	52.74	52.01	-0.29	4.3	3
405800	1663	5.2	-31.1	52.67	49.63	-0.06	4.6	-
401603	2718	24.0	-22.8	52.77	49.19	-0.10	4.9	5
405442	9	-30.3	9.9	52.77	49.72	-0.04	4.9	4
401221	892	-14.7	8.7	52.74	49.27	-0.25	5.1	11
401611	2589	-13.5	-0.1	52.74	48.77	0.21	5.1	9
406530	570	9.6	19.6	52.79	49.98	0.21	5.1	13
402692	2734	32.0	-21.8	52.53	51.75	-0.11	5.3	7
-	Typical σ	9	7	0.1	1.1	0.08	-	-
-	Signal	0	0	52.82	52.83	0	-	-

In-time RDC hit; Not used in CCA

MEG II Current Status

- Figure shows the effective number of muons accumulated for 2021-2023
- Accumulated data is already 9x that of the 2021 result
- The sensitivity after the full 2023 run (December) should approach the goal of the MEG II experiment, expected to reach a sensitivity of ~$9*10^{-14}$

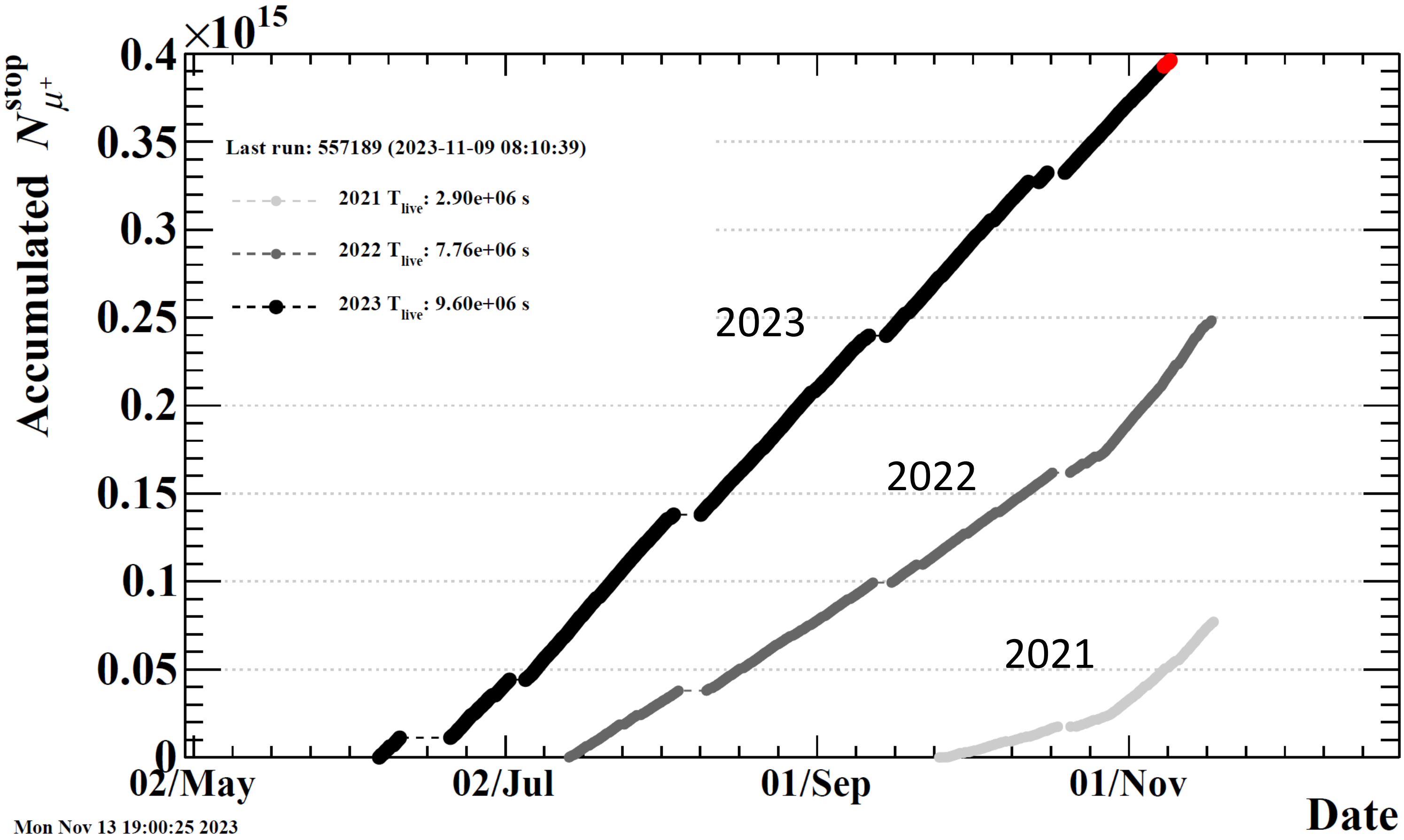

Conclusions

- MEG II collaboration has come a long way in the last few years. In the 2020 engineering run, the drift chamber experienced high currents and only a small fraction of the electronics were available
- In the 2021 physics run, the experiment achieved resolutions comparable to the MEG II design
- Now the 2021-2023 dataset is expected to achieve the most stringent limit on the CLFV $\mu \to e\gamma$ decay or detect a signal
- Will continue optimizing for 2022,2023 physics analysis. Focus on shortcomings:
  - Optimize the magnetic field calculation/measurements
  - Alternative LXe energy calculations
  - Alternative CDCH track finders
- Physics paper, Operations paper

Thanks for listening! Questions?

Backup: Normalization

$$N_{e\nu\bar{\nu}} = \frac{N^{\mu}_{e\nu\bar{\nu}}}{P_{e\nu\bar{\nu}}} \cdot \mathcal{B}_{e\nu\bar{\nu}} \cdot f_{e\nu\bar{\nu},*} \cdot T_{e\nu\bar{\nu}} \cdot \epsilon^{e\nu\bar{\nu}}_{TRG} \cdot \epsilon^{e\nu\bar{\nu}}_{e}$$

$$N_{e\gamma} = \frac{N^{\mu}_{e\gamma}}{P_{e\gamma}} \cdot \mathcal{B}_{e\gamma} \cdot T_{e\gamma} \cdot \epsilon^{e\gamma}_{TRG} \cdot \epsilon^{e\gamma}_{e} \cdot A^{\gamma}_{e\gamma} \cdot \epsilon^{e\gamma}_{\gamma} \cdot \epsilon^{e\gamma}_{SEL}$$

$$\frac{\mathcal{B}_{e\gamma}}{\mathcal{B}_{e\nu\bar{\nu}}} = \frac{N_{e\gamma}}{N_{e\nu\bar{\nu}}} \cdot \frac{f_{e\nu\bar{\nu},*}}{P_{e\nu\bar{\nu}}} \cdot \frac{\epsilon^{e\nu\bar{\nu}}_{TRG}}{\epsilon^{e\gamma}_{TRG}} \cdot \frac{\epsilon^{e\nu\bar{\nu}}_{e}}{\epsilon^{e\gamma}_{e}} \cdot \frac{1}{A^{\gamma}_{e\gamma}} \cdot \frac{1}{\epsilon^{e\gamma}_{\gamma}} \cdot \frac{1}{\epsilon^{e\gamma}_{SEL}}$$

$$SES = \frac{1}{N_{e\nu\bar{\nu}}} \cdot \frac{f_{e\nu\bar{\nu},*}}{P_{e\nu\bar{\nu}}} \cdot \frac{\epsilon^{e\nu\bar{\nu}}_{TRG}}{\epsilon^{e\gamma}_{TRG}} \cdot \frac{\epsilon^{e\nu\bar{\nu}}_{e}}{\epsilon^{e\gamma}_{e}} \cdot \frac{1}{A^{\gamma}_{e\gamma}} \cdot \frac{1}{\epsilon^{e\gamma}_{\gamma}} \cdot \frac{1}{\epsilon^{e\gamma}_{SEL}}$$

$$N_{\mu} = N_{e\nu\bar{\nu}} \cdot \frac{P_{e\nu\bar{\nu}}}{f_{e\nu\bar{\nu},*}} \cdot \frac{\epsilon^{e\gamma}_{TRG}}{\epsilon^{e\nu\bar{\nu}}_{TRG}} \cdot \frac{\epsilon^{e\gamma}_{e}}{\epsilon^{e\nu\bar{\nu}}_{e}} \cdot A^{\gamma}_{e\gamma} \cdot \epsilon^{e\gamma}_{\gamma} \cdot \epsilon^{e\gamma}_{SEL}$$

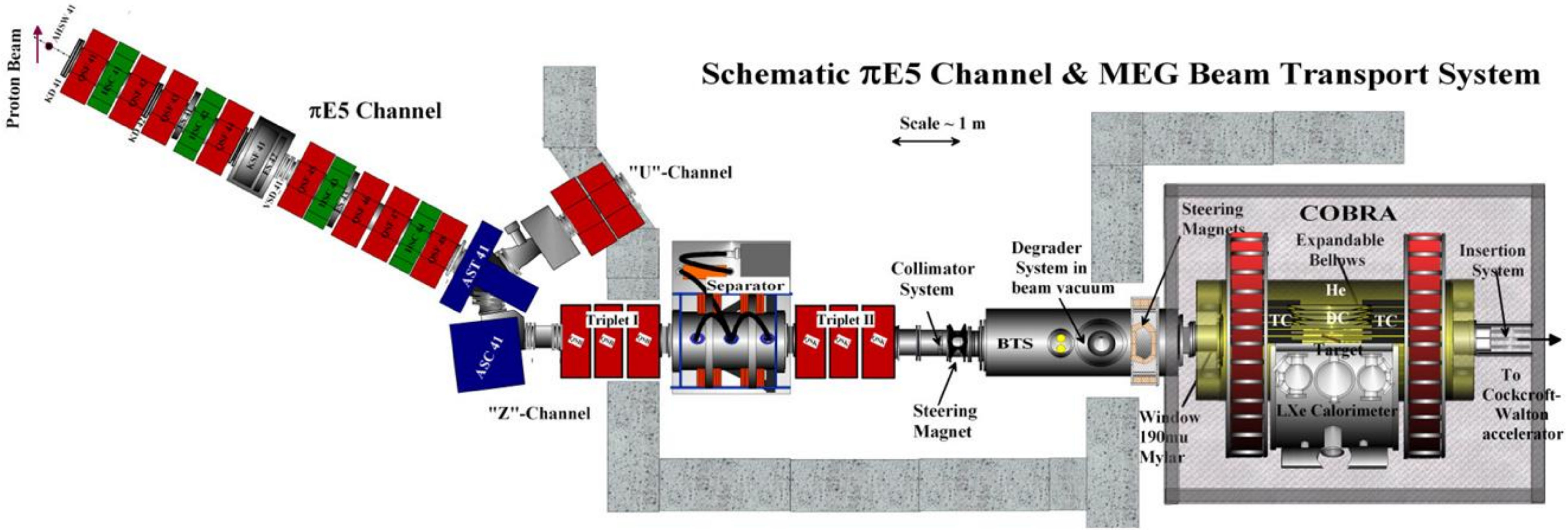

Figure 4 MEG Beam line with the πE5 channel and MEG detector system incorporated in and around the COBRA magnet.

- Anneal MPPCs every year in order to recover MPPC quantum efficiency
- Quantum efficiency degrades with beam exposure
- Likely related to removing a protective coating, removed to absorb VUV light on MPPCs
- Anneal using Joule method: i.e. applying high current

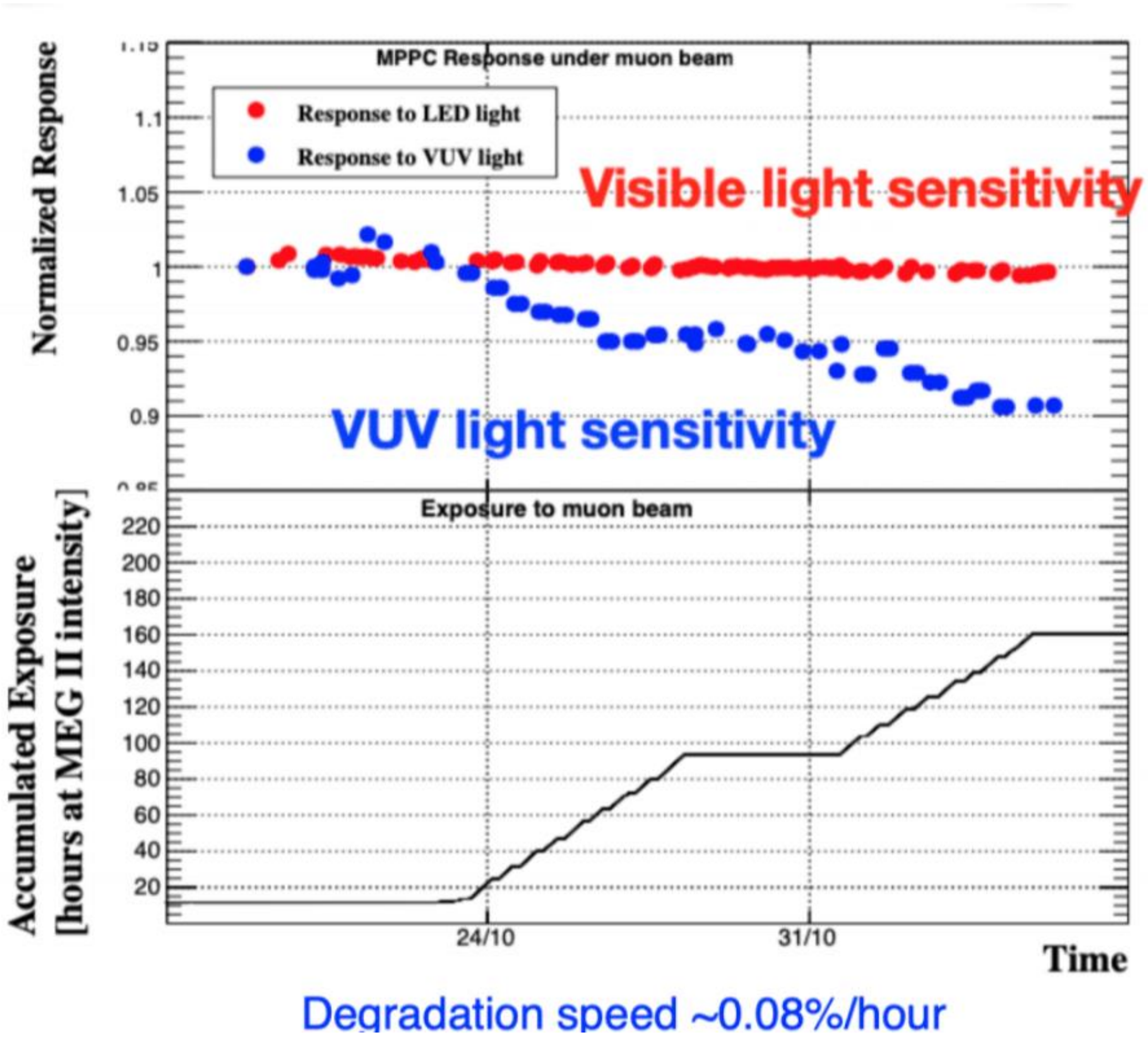

Backup: Camera Analysis

- Expect target motion on a short time scale e.g., following target insertions/extractions (LXe calibrations)
- ~120 dots printed on target surface; imaged by photographic camera ~1.2 m from target
- Image analysis code measures dot coordinates on the CCD
- Fit for the 3D target position, rotation, shape using projection equations: $X_{CCD} = \frac{f * X_{CAM}}{Z_{CAM} - f}$
- Analysis requires relative CDCH-target position

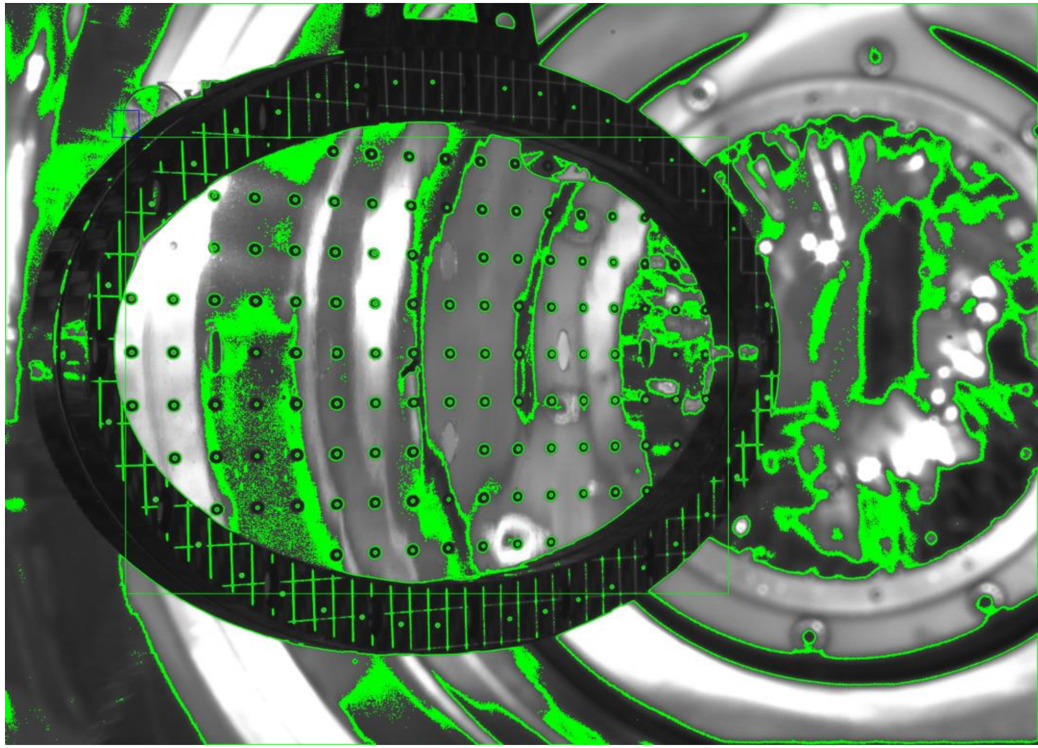

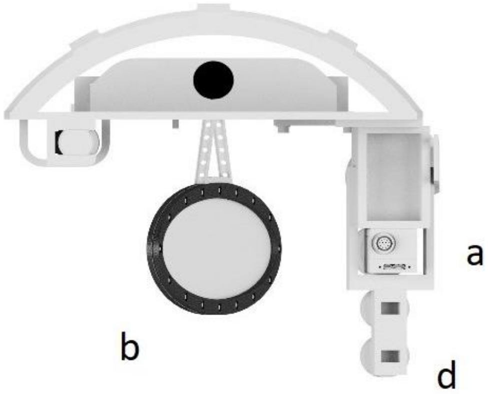

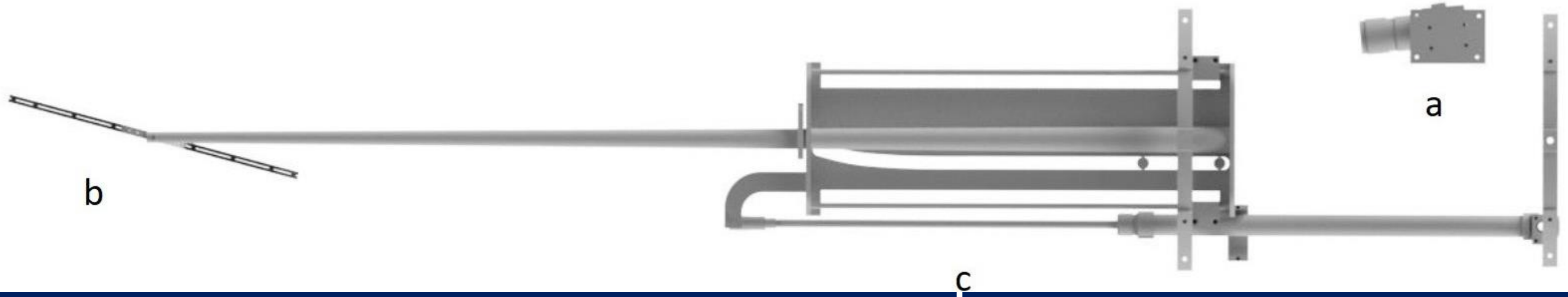

Backup: Target Survey + CT Scan

- Three optical corner cubes on the target frame
- Optical survey provides the corner position in relative to detectors (CDCH,LXe, etc.)
- Target CT scan provides the relative coordinates of the target foil/corner cubes in a nominal coordinates system
- Combination yields the relative position of the target foil with respect to the detectors at the time of the survey

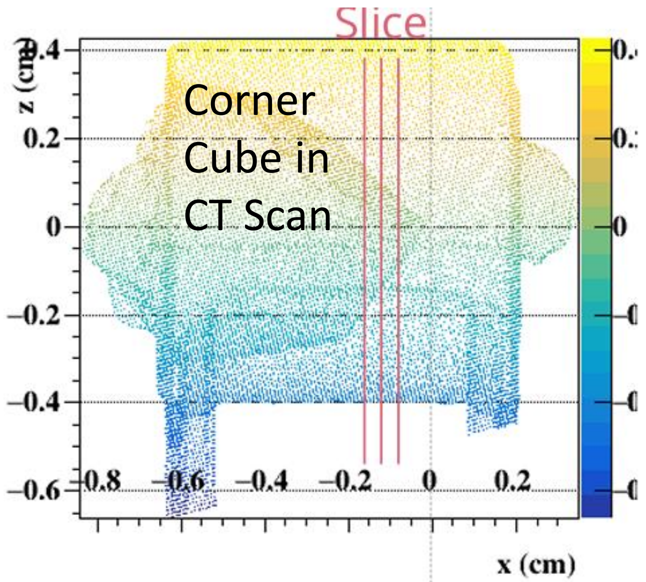

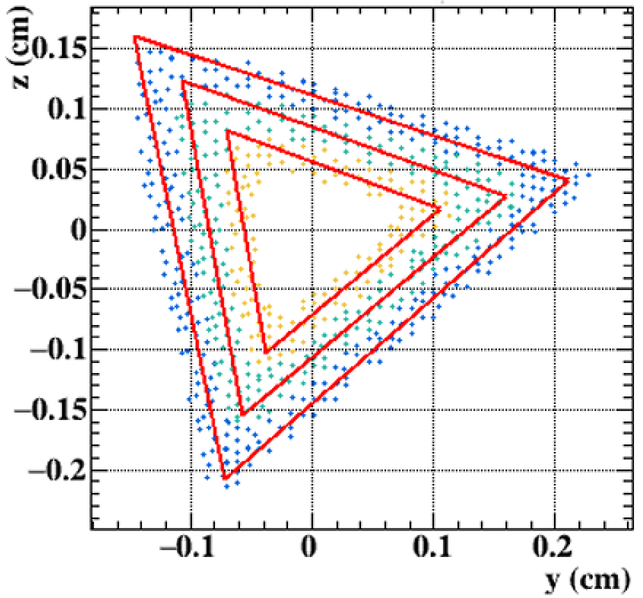

Backup: Camera Analysis Result

- Rigid body 6-parameter transformation: survey→ MEG data start (0→1000 h)
- ~600 μm shifts normal to the target surface: $\cos(15°)X_{MEG}$ + $\sin(15°)Z_{MEG}$
- Unknown origin, but significant work in area
- Reminder:

  600 μm → ~7 mrad φ_e error
- Small shifts of ~ 50 μm with insertions/extractions

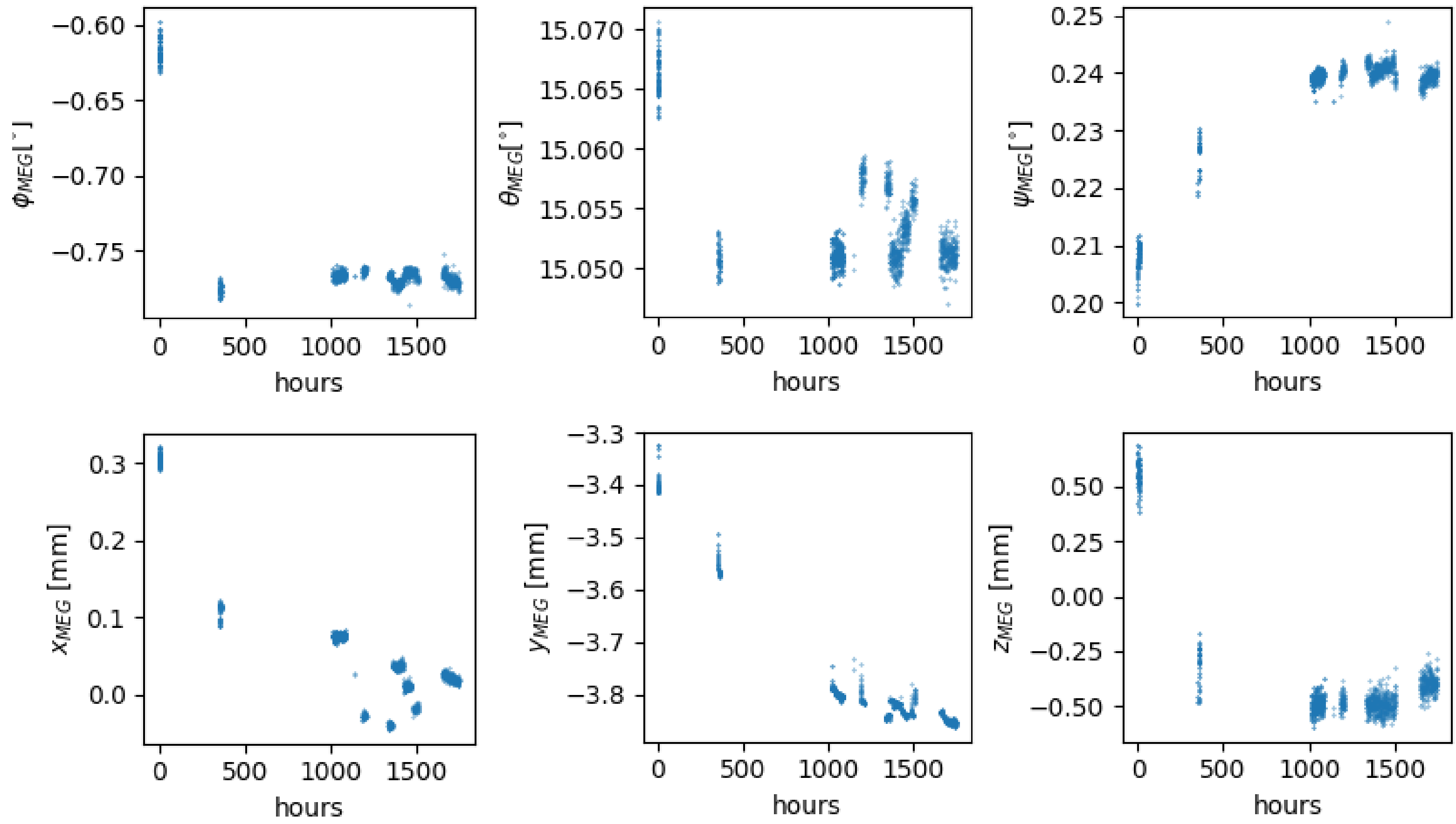

Backup: Target Shape

- CT scan and camera analysis shape agree within ~50 μm at all points on the surface
- Implement target into MEG analysis framework by tessellating the deformation into an array of triangular faces
- Propagate positrons to tessellation

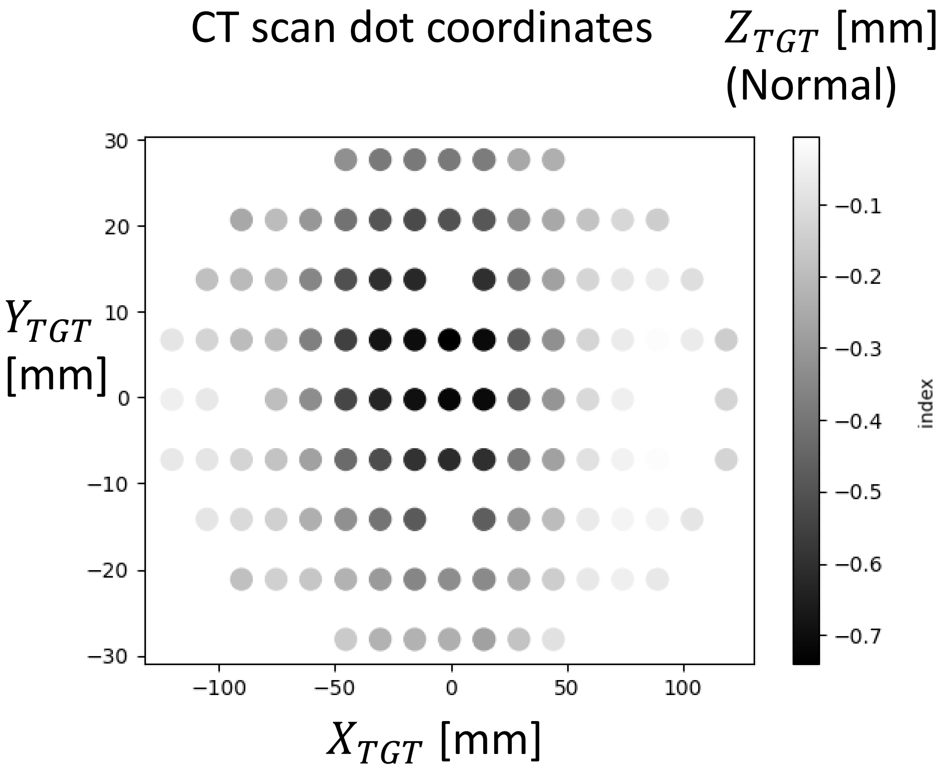

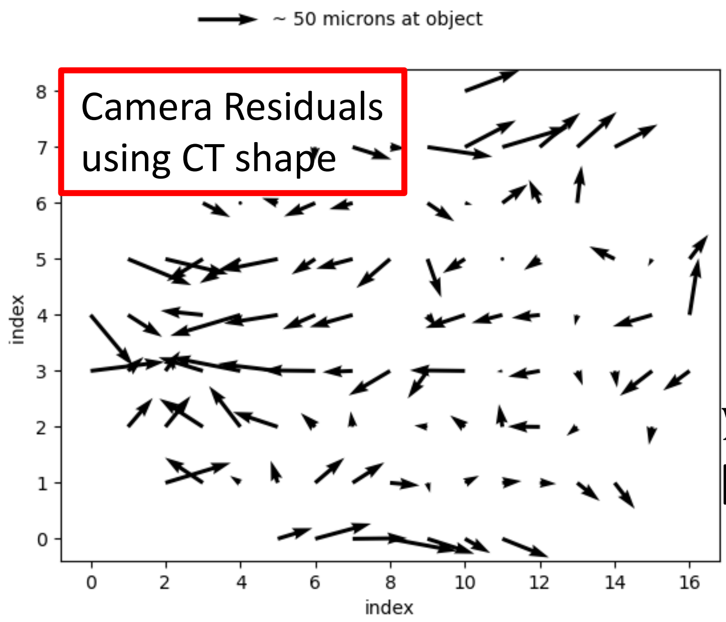

Backup: pTC Time Resolution

- pTC $\sigma_{t_{e^+}}$ estimated by comparing time of even/odd ordered hits in the same “cluster” of SPX hits
- Fit for $\sigma_{t_{e^+}}(N_{TC}) = \frac{112}{\sqrt{N_{TC}}}$
- Signal e^+ <N_{TC}> ~9

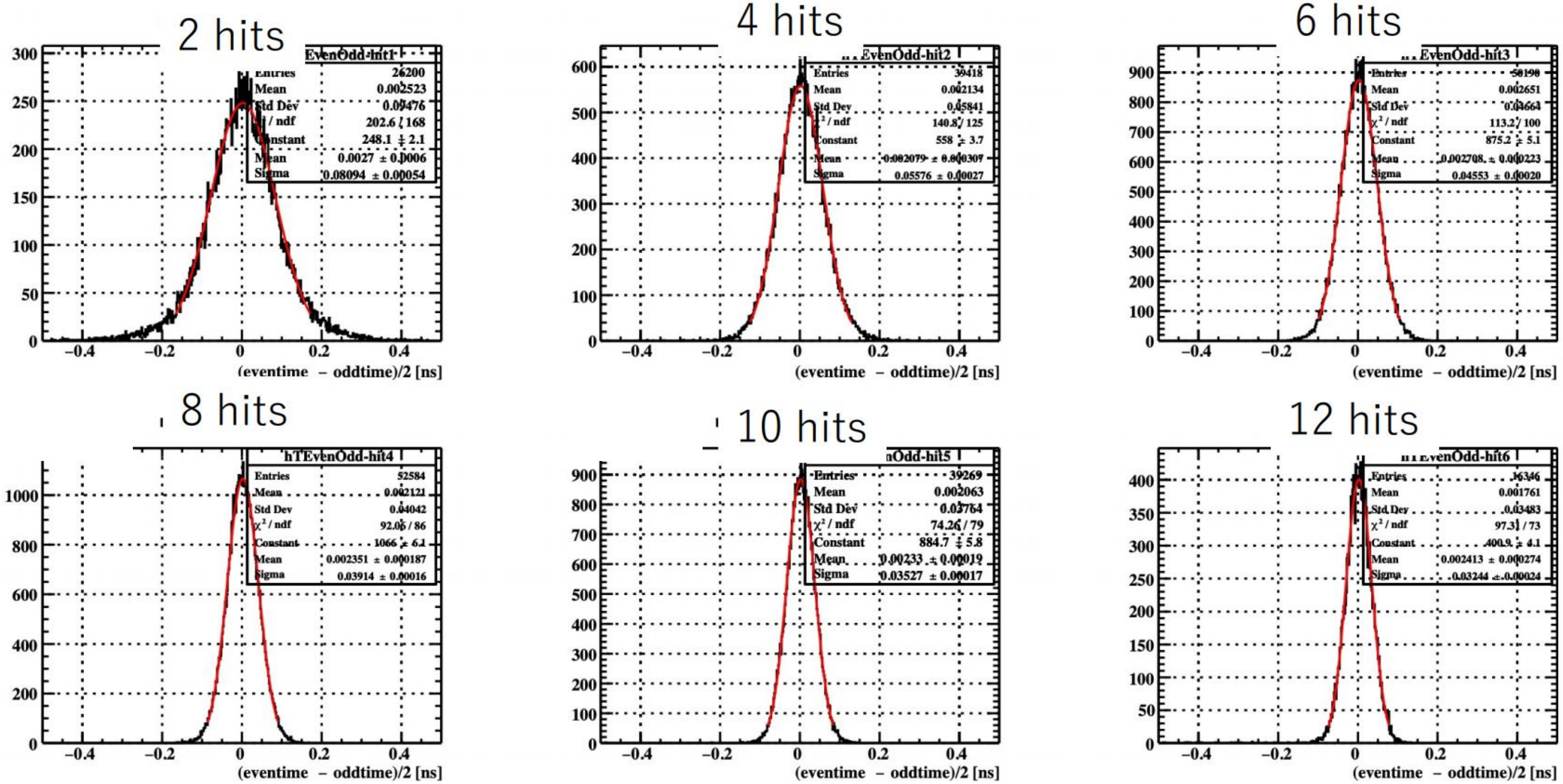

Kinematics/ Core σ	MEG I	MEG II Goal	MEG II 2021
t_{e+} (ps)	70	30	37

Positron Analysis

Physics Analysis

- Goal: detect the $\mu^+ \to e^+\gamma$ signal or calculate an upper-limit on BR of $\mu^+ \to e^+\gamma$ using $E_\gamma, E_e, \varphi_{e\gamma}, \theta_{e\gamma}, t_{e\gamma} + (t_{RDC-LXE}, E_{RDC})$
- Two **blind** physics analyses discussed in next few slides:
  - Cut and count analysis (2 separate analyses)
  - Maximum likelihood analysis (2 separate analyses)
- Common requirements:
  - **Calibrations, alignments, noise suppression**
  - **Positron/photon selection**
  - **Kinematic resolution estimates**
  - Correlations between kinematics
  - Both opt to include event-by-event information
  - **Estimates of background rates/distributions**

NN Track Selection Trained Directly On Data
To Remove Mismeasured Tracks

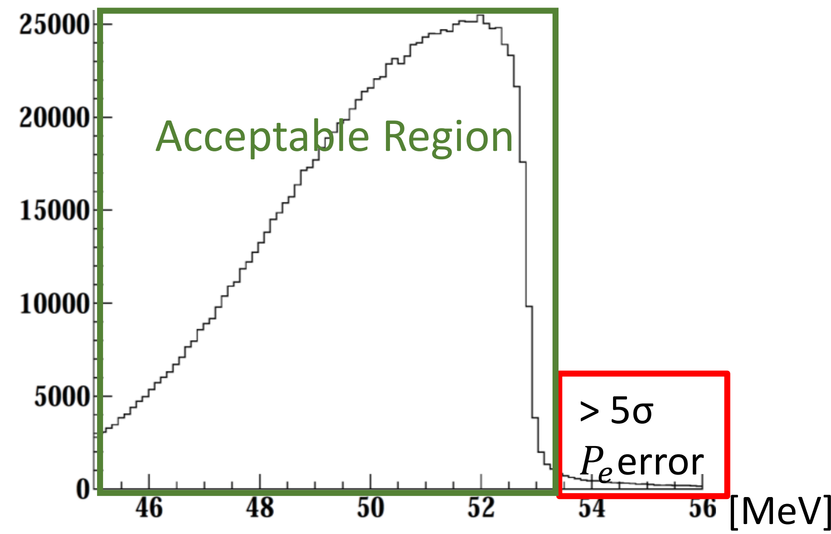

NN Accuracy with Varying Inputs

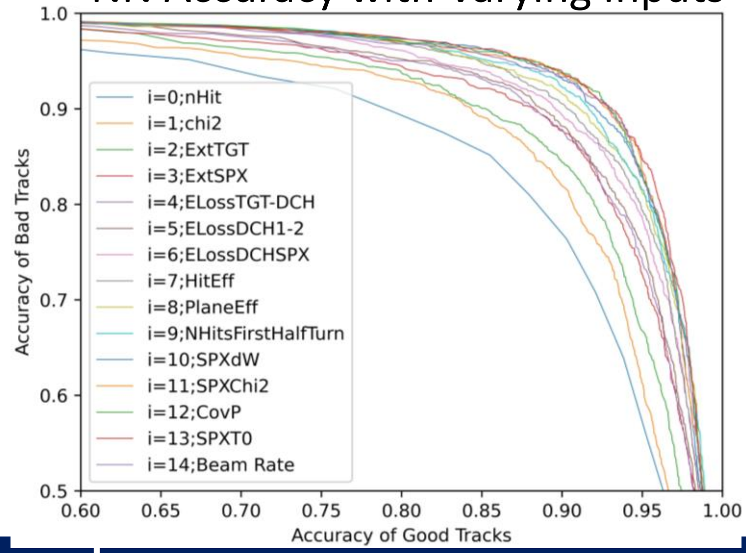

Backup: Positron Kinematic Correlations

- The double turn analysis also extracts correlations between kinematic variables
- Some are not accessible in the data and thus rely on MC
- Correlations:

$$\delta\phi = [p_0^{\phi} + p_1^{\phi} \cdot tan(\phi)] \cdot \delta E*$$

$$\delta Y = p_0^{Y} + p_1^{Y} \cdot \delta E*$$

$$\delta Z = [p_2^{Z} + p_3^{Z} \cdot cot(\theta)] \cdot \delta E*$$

$$\delta Z = p_0^{Z} + p_1^{Z} \cdot \delta\theta$$

$$\delta\phi = [p_5^{\phi} + p_6^{\phi} \cdot \phi + p_7^{\phi} \cdot \phi^2] \cdot \delta Z*$$

$$\delta\phi = [p_2^{\phi} + p_3^{\phi} \cdot \phi + p_4^{\phi} \cdot \phi^2] \cdot \delta\theta$$

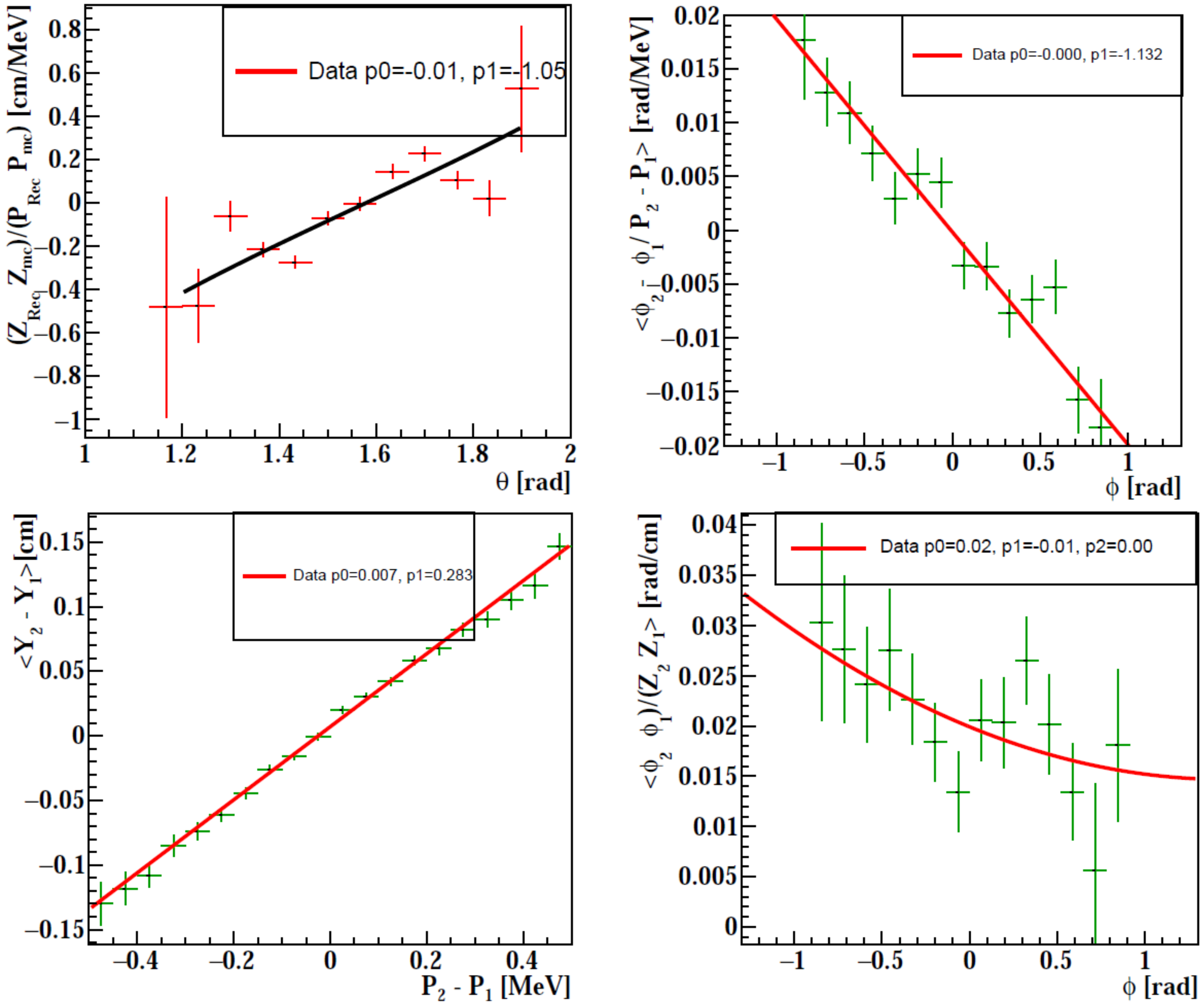

- Model-independent effective Lagrangian with two types of theoretical models
- If (e.g. SUSY, κ<<1):
  BR(μ → eγ) ~ BR(μN→eN)/α
- If (e.g. leptoquarks, κ>>1):
  μN→eN is at tree level and μ→eγ is at loop level
- Mu2e reaches far lower sensitivities in the quark-lepton coupling models
- MEG II and Mu2e are synergetic: in κ<<1 models the two will have a comparable sensitivity
  (if MEG II sees a signal, Mu2e should too)

$$\mathcal{L}_{\rm CLFV} = \frac{m_\mu}{(\kappa+1)\Lambda^2}\bar{\mu}_R\sigma_{\mu\nu}e_L F^{\mu\nu} + h.c.$$
$$\frac{\kappa}{(1+\kappa)\Lambda^2}\bar{\mu}_L\gamma_\mu e_L\left(\bar{u}_L\gamma^\mu u_L + \bar{d}_L\gamma^\mu d_L\right) + h.c.$$

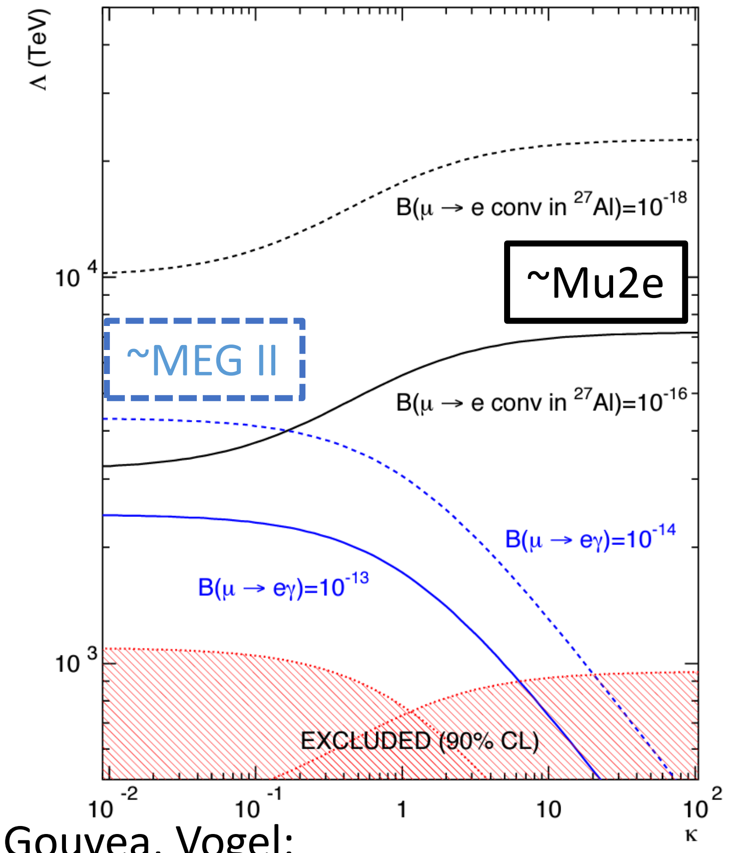

de Gouvea, Vogel: https://doi.org/10.1016/j.ppnp.2013.03.006

Backup: XEC Calibrations

Process		Energy	Main Purpose	Frequency
Cosmic rays	μ^+ from atmospheric showers	Wide spectrum $\mathcal{O}$(GeV)	LXe–CDCH relative position LXe purity	Annually On demand
Charge exchange	$\pi^- p \to \pi^0 n$ $\pi^0 \to \gamma\gamma$	55, 83, 129 MeV photons	LXe energy scale/resolution	Annually
Radiative μ–decay	$\mu^+ \to e^+ \nu \bar{\nu} \gamma$	Photons >40 MeV, Positrons >45 MeV	LXe–pTC relative timing	Continuously
Proton accelerator	${}^7\mathrm{Li}(p,\gamma){}^8\mathrm{Be}$ ${}^{11}\mathrm{B}(p,\gamma){}^{12}\mathrm{C}$	14.8, 17.6 MeV photons 4.4, 11.6, 16.1 MeV photons	LXe uniformity/purity LXe–pTC timing	Weekly Weekly
Neutron generator	${}^{58}\mathrm{Ni}(n,\gamma){}^{59}\mathrm{Ni}$	9 MeV photons	LXe energy scale	Weekly
Radioactive source	${}^{241}\mathrm{Am}(\alpha,\gamma){}^{237}\mathrm{Np}$	5.5 MeV α's	LXe PMT/SiPM calibration LXe purity	Weekly
Radioactive source	${}^9\mathrm{Be}(\alpha_{^{241}\mathrm{Am}}, n){}^{12}\mathrm{C}^\star$ ${}^{12}\mathrm{C}^\star(\gamma){}^{12}\mathrm{C}$	4.4 MeV photons	LXe energy scale	On demand
Radioactive source	${}^{57}\mathrm{Co}(EC,\gamma){}^{57}\mathrm{Fe}$	136 (11 %), 122 keV (86 %) X-rays	LXe–spectrometer alignment	Annually
LED		UV region	LXe PMT/SiPM calibration	Continuously

- Observed low frequency noise on the CDCH waveforms coherent over entire electronics chips
- Developed algorithms to suppress noise by averaging the voltage bin-by-bin/chip away from signals
- **Noise suppression is critical to improving hit efficiency and improving track space-point measurements**

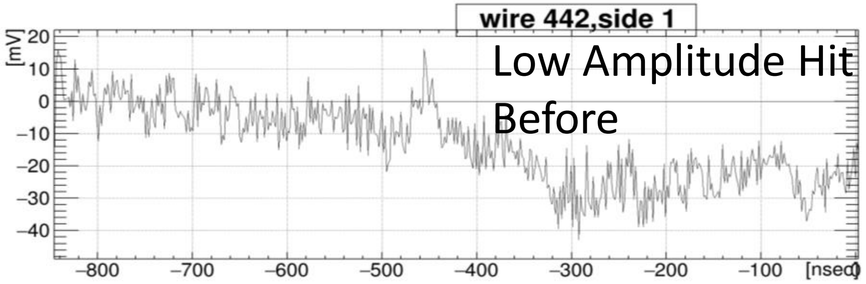

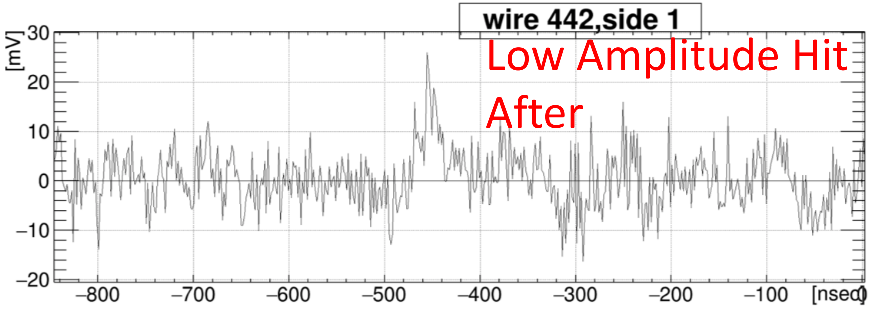

Noise Spectra

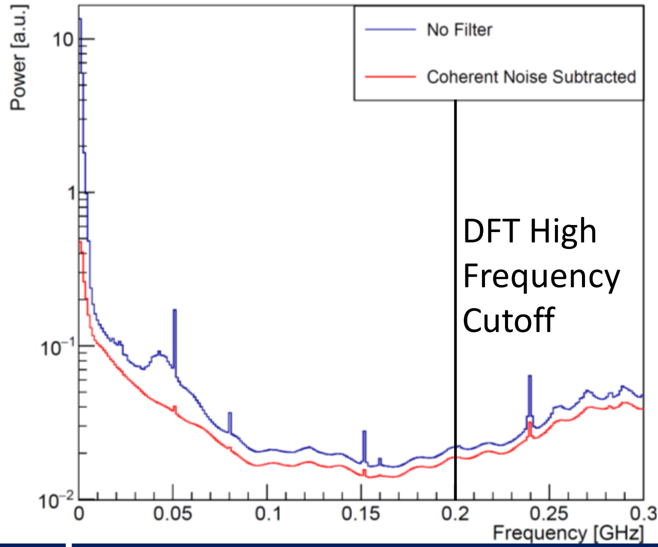

Backup: XEC Energy Calibration